

# Scaffold-Hopping and Structure-Based Discovery of Potent, Selective, And Brain Penetrant *N*-(1*H*-Pyrazol-3-yl)pyridin-2-amine Inhibitors of Dual Leucine Zipper Kinase (DLK, MAP3K12)

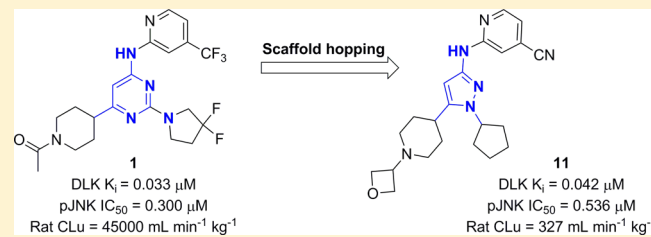
Snahel Patel,<sup>\*,†</sup> Seth F. Harris,<sup>\*,§</sup> Paul Gibbons,<sup>†</sup> Gauri Deshmukh,<sup>⊥</sup> Amy Gustafson,<sup>∇</sup> Terry Kellar,<sup>†</sup> Han Lin,<sup>‡</sup> Xingrong Liu,<sup>⊥</sup> Yanzhou Liu,<sup>†</sup> Yichin Liu,<sup>∇</sup> Changyou Ma,<sup>#</sup> Kimberly Searce-Levie,<sup>‡</sup> Arundhati Sengupta Ghosh,<sup>‡</sup> Young G. Shin,<sup>⊥,○</sup> Hilda Solanoy,<sup>‡</sup> Jian Wang,<sup>#</sup> Bei Wang,<sup>‡,◆</sup> Jianping Yin,<sup>§</sup> Michael Siu,<sup>†</sup> and Joseph W. Lewcock<sup>‡</sup>

<sup>†</sup>Departments of Discovery Chemistry, <sup>§</sup>Structural Biology, <sup>‡</sup>Neurosciences, <sup>⊥</sup>Drug Metabolism and Pharmacokinetics, <sup>∇</sup>Biochemical and Cellular Pharmacology, Genentech, Inc., 1 DNA Way, South San Francisco, California 94080, United States

<sup>#</sup>Department of Chemistry, WuXi AppTec Co., Ltd., 288 Fute Zhonglu, Wai Gao Qiao Free Trade Zone, Shanghai, 200131, P. R. China

## Supporting Information

**ABSTRACT:** Recent data suggest that inhibition of dual leucine zipper kinase (DLK, MAP3K12) has therapeutic potential for treatment of a number of indications ranging from acute neuronal injury to chronic neurodegenerative disease. Thus, high demand exists for selective small molecule DLK inhibitors with favorable drug-like properties and good CNS penetration. Herein we describe a shape-based scaffold hopping approach to convert pyrimidine **1** to a pyrazole core with improved physicochemical properties. We also present the first crystal structures of DLK. By utilizing a combination of property and structure-based design, we identified inhibitor **11**, a potent, selective, and brain-penetrant inhibitor of DLK with activity in an in vivo nerve injury model.



## INTRODUCTION

There has been longstanding interest in the development of c-Jun N-terminal kinase (JNK) pathway inhibitors for the treatment of neurodegenerative disease due to the potent neuroprotection observed in multiple contexts following attenuation of JNK signaling.<sup>1,2</sup> Dual leucine zipper kinase (DLK, MAP3K12) is an upstream regulator of JNK signaling whose expression is enriched in neurons.<sup>3,4</sup> Recent work has demonstrated that DLK regulates stress-induced JNK signaling following neuronal injury and therefore represents an attractive approach for modifying JNK activity in the central nervous system (CNS).<sup>5,6</sup> Consistent with this idea, genetic deletion or pharmacological inhibition of DLK is sufficient to provide considerable protection of neurons from degeneration in a variety of in vitro and in vivo models, suggesting this kinase represents an attractive therapeutic target.<sup>5–12</sup>

We recently disclosed the first potent, selective, and brain-penetrant compounds specifically designed to inhibit DLK. The lead inhibitor **2** (GNE-3511, Figure 1, Approach 1), displayed protection of primary neurons in an in vitro axon degeneration assay as well as activity in the mouse models of glaucoma/optic neuropathy (optic nerve crush) and Parkinson's disease (MPTP) after oral dosing.<sup>13</sup> Despite the attributes of **1** and **2**, these compounds suffered from poor physicochemical properties leading to high free (unbound) clearances (Table

6). To address this, a parallel scaffold hopping<sup>14,15</sup> strategy was adopted (Figure 1, Approach 2) in order to improve the properties of these compounds for development toward a potential therapeutic.<sup>16</sup>

## RESULTS AND DISCUSSION

To gain a specific and detailed understanding of the binding mode of our inhibitors, we determined the novel crystal structure of the DLK kinase domain with and without bound ligands. The protein shows the expected canonical kinase fold, with the ATP binding site interposed between a smaller N-terminal subdomain and a larger, predominantly  $\alpha$ -helical C-terminal lobe (Figure 2). In the common model of kinase activation, phosphorylation events trigger concerted motions of the activation loop, helix C, and the conserved DFG motif.<sup>17–19</sup> Active kinase conformations are characterized by a DFG “in” orientation with concomitant formation of a salt bridge between an N-terminal lysine (DLK Lys152) and its partner acidic residue on helix C. In our apo DLK structure, the activation loop is ordered including an  $\alpha$ -helical segment at its C-terminal region (residues 264–274). The DFG motif (residues 254–256) has an active-like “in” conformation;

Received: July 9, 2015

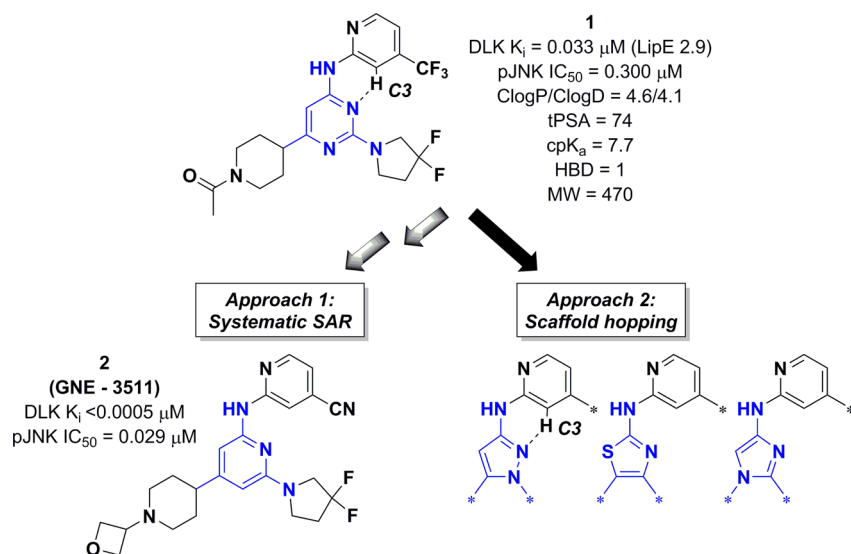


**Figure 1.** Pyrimidine core **1** a key juncture where Approaches 1 and 2 were developed in parallel. Approach 1 resulting in pyridyl core **2** as previously reported. Approach 2 shows the intramolecular aminopyridine C3–H interaction with pyrazole core N2 giving an example of a planar system retained when compared to compound **1**.

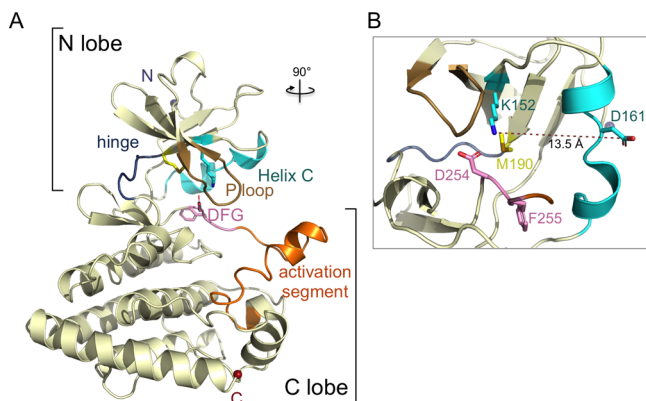


**Figure 2.** Apo crystal structure of the DLK kinase domain shows an ordered activation segment, a DFG-in type conformation, and an unusual disrupted helix C. (A) The canonical kinase N- and C-terminal lobes are labeled with conserved features colored: interdomain hinge (navy), glycine-rich P-loop (brown), helix C (cyan), conserved N-lobe Lys152 (cyan), gatekeeper Met190 (yellow), DFG motif (pink), activation loop (orange). (B) An active site view shows the DFG motif (pink) “in” conformation, while the active-kinase N-lobe Lys152 to helix C Asp161 salt bridge is not formed. DLK’s unusual helix C Asp161 substitution (instead of conserved Glu) is conspicuously turned out from the body of the kinase and disrupts the helical secondary structure, creating a 13.5 Å gap between the putative activation partners (see Supporting Information Figure S1 for electron density of this region).

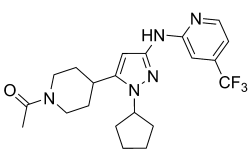
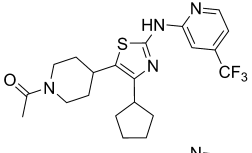
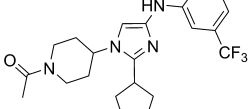
however the helix C salt bridge is not formed. DLK is unusual in that the highly conserved acidic Glu of helix C is replaced by an Asp substitution. This Asp161 is part of an unexpected kink of the secondary structure that disrupts the  $\alpha$ -helix orienting the acidic side chain of this residue away from the body of the kinase,  $\sim 13$  Å from its putative partner Lys152 (see Figure S1 of the Supporting Information). A lack of any crystal symmetry mates in the vicinity suggests the conformation is not artifactual. Given the important role of helix C in kinase activation and the consistent disposition across all of our DLK structures, this disrupted and inverted Asp conformation is

notable, though it remains unclear what specific role this highly unusual variation would have in the physiological environment.

The ATP binding pocket is characterized by the classical kinase hinge backbone pattern of hydrogen-bond interactions on one side, while the malleable glycine-rich, “P-loop” motif (residues 129–142) shapes both the upper surface and opposite wall of the cavity. The back region is affected by side chain positions of the gatekeeper Met190 and the catalytic Asp254. The binding cleft widens to the “front” toward greater solvent exposure in the context of our truncated kinase domain construct. This novel kinase structure serves to elucidate key relationships of the conserved architecture and as an important tool to guide structure-based drug design. The interactions of our inhibitors with these features are further described below, specifically contact to DLK’s adaptable P-loop as we designed these alternate scaffolds.

Our starting point, as exemplified by **1** (DLK  $K_i$  = 0.033  $\mu$ M, p-JNK  $IC_{50}$  = 0.300  $\mu$ M, clogP 4.6, tPSA 74 Å<sup>2</sup>, HBD 1, LipE 2.9) has low lipophilic ligand efficiency<sup>16,20</sup> and poor physiochemical properties that led to high rat-free clearance (CL<sub>r</sub>) and low free drug exposure (Table 6). In an attempt to improve this, we took an alternative approach by investigating a shape-based scaffold hopping strategy<sup>21</sup> with the goal of replacing the central pyrimidine core with five-membered heterocycles.<sup>22</sup> From our assessment, the pyrazole, thiazole, and imidazole isomers shown in Figure 1 can maintain the required coplanar subunit similar to *N*-(pyridin-2-yl)pyrimidin-4-amine **1** (see Figure S2 of the Supporting Information). Further elaboration of these analogs by the inclusion of functional groups to extend toward the P-loop and solvent led us to the compounds highlighted in Table 1. While each system had comparable TanimotoShape and TanimotoCombo scores,<sup>23,24</sup> we initiated chemistry efforts with the pyrazole core based on synthetic tractability to expand SAR under the P-loop and solvent regions. Attention to properties necessary for brain penetration (HBD < 2, tPSA < 90 Å<sup>2</sup>, CNS MPO > 4),<sup>25,26</sup> while tracking improvements to lipophilic efficiency, was important to our chemistry efforts. Additionally, selectivity against the JNK pathway kinases (DLK → MKK4/7 → JNK2/3

Table 1. ROCS Shape-Overlay Analysis<sup>a</sup>

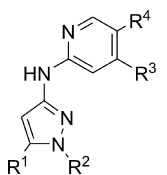
Structure Query	TanimotoShape	TanimotoCombo
	0.777	1.318
	0.749	1.311
	0.754	1.246

<sup>a</sup>To assess core replacements, a model based on the subunit 2,6-dimethyl-*N*-(4-(trifluoromethyl)pyridin-2-yl)pyrimidin-4-amine bioactive conformation was obtained by generation of the lowest-energy conformation for five-membered heterocyclic systems (pyrazole, thiazole, or imidazole) with OMEGA and subsequent quantum mechanical minimization at the B3LYP/6-31G\*\* level of theory (see [Supporting Information](#) for computational methods). The three heterocyclic replacements evaluating favorably through this analysis, *N*-(1,5-dimethyl-1*H*-pyrazol-3-yl)-4-(trifluoromethyl)pyridin-2-amine, 4,5-dimethyl-*N*-(4-(trifluoromethyl)pyridin-2-yl)thiazol-2-amine, and *N*-(1,2-dimethyl-1*H*-imidazol-4-yl)-4-(trifluoromethyl)pyridin-2-amine were scored using a ROCS shape-overlay aiming to retain global shape similarity with respect to elaborated compound 1. Expansion with the proposed P-loop and solvent side chains showed a suitable level of shape preservation with respect to compound 1 and similar TanimotoShape and TanimotoCombo scoring between the three heterocyclic systems.

→ cJun) and DLK homologues (MLK 1/2/3) was a prerequisite to in vivo evaluation.<sup>27</sup>

Starting with 1-isopropyl-5-(piperidin-4-yl)-1*H*-pyrazol-3-amine, we evaluated the C4 and C5 position of the aminopyridine hinge binder. Similar to the reported SAR of the pyrimidine series (1),<sup>13</sup> the 2-aminopyridine C4 substitution was optimal for potency (matched pairs compound 3,  $K_i = 0.145 \mu\text{M}$ /compound 5,  $K_i = >1.6 \mu\text{M}$  and compound 4,  $K_i = 0.160 \mu\text{M}$ /compound 6,  $K_i = >1.6 \mu\text{M}$ ) (Table 2). Furthermore, comparison of lipophilic efficiencies demonstrated that the 2-amino-4-cyanopyridine 4 (LipE 3.9) was superior to 2-amino-4-trifluoromethylpyridine 3 (LipE 2.6). Our X-ray structure of DLK complexed with trifluoromethylpyridine 3 confirmed that the binding mode is consistent with the calculated low-energy ligand conformation (see [Supporting Information](#) Figure S2 and Table S2) for the pyrazole group replacement (Figure 3). The central pyrazole core and pyridine ring lie on the platform of the C lobe Gly196 and Leu243, with hydrogen bonds formed between the ligand and backbone carbonyl and amide atoms of the hinge residue Cys193. In addition, the pyridine C6–H contributes to a noncanonical hydrogen bond with the Glu191 backbone carbonyl. The core pyrazole ring is also aligned to participate in  $\pi$  orbital interactions with the side chain of Phe192, and the piperidine moiety extends to the front solvent-exposed opening. In contrast to the apo example, the activation segment is disordered in our ligand-bound structures (residues 257–

269), while the outward, helix-disrupting orientation of helix C Asp161 is maintained. The trifluoromethyl moiety makes van der Waals contacts with the Met190 gatekeeper residue and with Val139. To accommodate the trifluoromethyl and isopropyl groups, the P-loop is lifted slightly relative to the apo structure and bent more sharply at residues Ser133 and Ala138 such that the tip drapes over the outer edge of the ligand to form an enclosed cavity. The P-loop tip Gln136 is stabilized adjacent to the ligand trifluoromethyl group via a hydrogen bond to Ser253 and packs between the conserved kinase residues Lys152 and the catalytic Asp254. Further evaluation under the P-loop led us to introduce the proposed cyclopentyl group from our ROCS analysis at pyrazole N1 (Table 1), with the aim to occupy available space observed in the structure and increase van der Waals interactions (for example with Gly132) for improved potency. Satisfyingly trifluoromethylpyridine 7 ( $K_i = 0.007 \mu\text{M}$ , p-JNK  $\text{IC}_{50} = 0.183 \mu\text{M}$ ) and cyanopyridine 8 ( $K_i = 0.022 \mu\text{M}$ , p-JNK  $\text{IC}_{50} = 0.188 \mu\text{M}$ ) showed improved biochemical potency and activity in a cell-based assay measuring levels of JNK phosphorylation (p-JNK) induced by DLK overexpression.<sup>13</sup> These results validated our strategy for the pyrazole core replacement. Consistently, the more polar cyanopyridine 8 (LipE 4.1) showed the best lipophilic efficiency. In a MDCK-MDR1 assay, 3 (BA/AB = 36) and 8 (BA/AB = 95) are efflux substrates despite low tPSA ( $<80 \text{ \AA}^2$ ) due to a basic amine. Holding the hinge binder constant to the more lipophilic efficient 2-aminoisonicotinonitrile moiety, we then investigated capping the piperidine N4 to reduce the hydrogen-bond donor count and basicity in order to improve permeability. Small capping groups such as acyl and oxetane, compounds 9 ( $K_i = 0.44 \mu\text{M}$ , MDRI-MDCK BA/AB = 9.1) and 10 ( $K_i = 0.549 \mu\text{M}$ , MDRI-MDCK BA/AB 1.9), respectively, showed that the oxetane moiety improved efflux liability.<sup>13</sup> Combining this result with the pyrazole N1 cyclopentyl side chain from compound 8 gave us 11, where a desirable balance of potency and efflux properties was realized ( $K_i = 0.042 \mu\text{M}$  and p-JNK  $\text{IC}_{50} = 0.536 \mu\text{M}$ , MDRI-MDCK BA/AB 1.4, AB  $8.8 \times 10^{-6} \text{ cm/s}$ ). Our crystal structure of 11 bound to DLK supported these designs (Figure 4). The core of the scaffold is very closely matched to 3, with consistent position of the protein features and core-interacting side chains. The cyano group extends into the back region near residues Lys152, Val139, and Gln136. The introduced cyclopentyl group maintains a similar DLK P-loop conformation as observed with 3, but the greater bulk causes a small additional shift upward and outward. The distal oxetane capping group extends, as expected, away from the protein into the less constrained solvent-accessible environment, permitting more facile modulation of ligand properties. Based on these results we looked to improve potency by further extending the pyrazole N1 SAR under the P-loop and holding the 2-((5-(1-(oxetan-3-yl)piperidin-4-yl)-1*H*-pyrazol-3-yl)amino)-isonicotinonitrile subunit constant (Table 3). The pyrazole N1-(3,3-difluorocyclopentyl) analog 12 showed comparable biochemical and in vitro microsomal data to 11 but diminished cellular potency (p-JNK  $\text{IC}_{50} = 0.721 \mu\text{M}$ ) and permeability (MDRI-MDCK BA/AB 5.8). Polarity under the P-loop was not well-tolerated. 1-(Tetrahydrofuran-3-yl) 13 resulted in a loss of biochemical potency with increased efflux liability ( $K_i = 0.378 \mu\text{M}$ , MDRI-MDCK BA/AB 7.6). Similarly ring expansion to 1-(tetrahydro-2*H*-pyran-4-yl) 14 showed a loss in potency and high efflux liability ( $K_i = 0.593 \mu\text{M}$ , MDRI-MDCK BA/AB 15). Extending under the P-loop with 1-

Table 2. Pyrazole N1 and C5-Substituent and Pyridine C4/C5-Substituent SAR<sup>a</sup>


Compound	R <sup>1</sup>	R <sup>2</sup>	R <sup>3</sup>	R <sup>4</sup>	K <sub>i</sub> (μM)	pJNK IC <sub>50</sub> (μM)	MDR1-MDCK BA/AB (AB) <sup>b</sup>	ClogP	tPSA	LipE <sup>c</sup>
3					0.145	-	36 (0.5)	4.2	54	2.6
4					0.160	-	- (-)	2.9	78	3.9
5					>1.6	-	- (-)	4.2	54	>1.6
6					>1.6	-	- (-)	3	78	>2.8
7					0.007	0.183	- (-)	4.8	54	3.3
8					0.022	0.188	95 (0.2)	3.6	78	4.1
9					0.44	>10	9.1 (2.1)	3	86	3.4
10					0.549	>10	1.9 (9.3)	3.1	79	3.2
11					0.042	0.536	1.4 (8.8)	3.7	78	3.7

<sup>a</sup>All assay results represent the geometric mean of a minimum of two determinations, and these assays generally produced results within 3-fold of the reported mean. <sup>b</sup>MDCK-MDR1 human P-gp transfected cell line. Basolateral-to-apical/apical-to-basolateral. Units =  $\times 10^{-6}$  cm s<sup>-1</sup>. <sup>c</sup>LipE =  $-\log K_i - \text{clogP}$ .

(cyclobutylmethyl) **15** retained potency ( $K_i = 0.133$  μM, p-JNK IC<sub>50</sub> = 1.4 μM) but not significantly. Finally we investigated SAR in the solvent exposed region by replacing *N*-oxetanylpiperidine **11** with *N*-oxetanylazetidine **16**, *N*-oxetanylpiperidine **17**, and furanyl **18**. In each case comparable biochemical and cellular potency to **11** was observed. Compounds **16** (MDR1-MDCK BA/AB 3.3, tPSA 79 Å<sup>2</sup>) and **17** (MDR1-MDCK BA/AB 3.7, tPSA 79 Å<sup>2</sup>) suffered from potential efflux liability. Compound **18** (MDR1-MDCK BA/AB 1) showed improved efflux liability but at the expense of metabolic stability in liver microsomes. Finally we evaluated the thiazole and imidazole core replacements outlined in Table 1. To reduce lipophilicity of the thiazole scaffold, the proposed cyclopentyl group (Table 1, clogP 5.3) was substituted with a cyclopropyl side-chain (clogP 4.5). Additionally, for both the thiazole and imidazole core replacements we replaced the 4-(trifluoromethyl)pyridin-2-amine with the 2-aminoisonicotinonitrile hinge binder and *N*-acetylpiperidine with the more favorable *N*-oxetanylpiperidine solvent exposed side-chain (TanimotoShape/TanimotoCombo 0.777/1.458 and 0.803/1.371, respectively, Table 4). Although the TanimotoShape and TanimotoCombo scoring were comparable between the five-membered heterocyclic replacements highlighted in Table 1

(pyrazole **11** [TanimotoShape/TanimotoCombo 0.819/1.509], thiazole **19** and imidazole **20**), the computational method correctly rank ordered the suitability of these core changes (pyrazole **11**  $K_i = 0.042$  μM > thiazole **19**  $K_i = 0.569$  μM >> imidazole **20**  $K_i > 1.6$  μM).

We compared the crystal structures of pyrazole **11** to that of DLK bound to pyridine **2** (Approach 1). The exact superposition of the 2-amino-4-cyanopyridine hinge binder of the inhibitors and the close alignment of the solvent exposed *N*-oxetanylpiperidine moieties is a testament to a successful design strategy incorporating the altered vectors emanating from the five- versus six-membered core ring differences (Figure 5). Both ligands have relatively large chemical moieties positioned under the P-loop resulting in very similar protein backbone conformations. Compound **2** positions a 3,3-difluoropyrrolidine (compared to cyclopentyl **11**) group that is likely connected to the upward-turned position of Gln136 relative to downward wrap around the ligand with **11** (Figure 5b), which in turn induces a small shift in the Asp254 rotamer. These minor adjustments illustrate that the DLK P-loop includes subtle as well as coarser conformational shifts in response to the different P-loop-oriented groups of the two ligands. These nuanced considerations underpin the well-



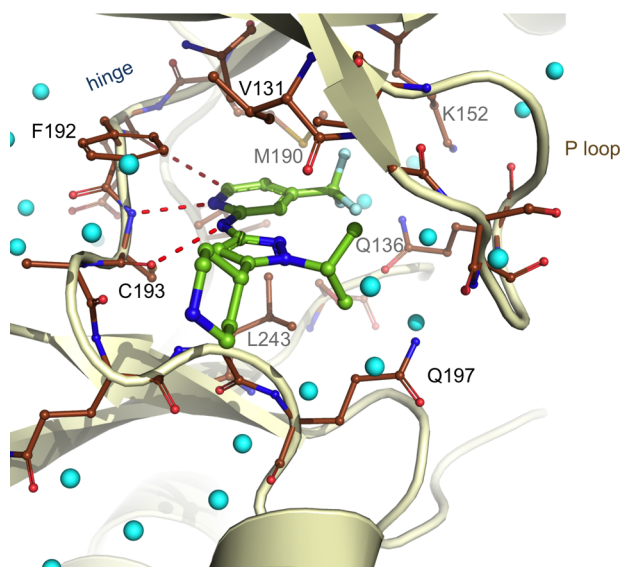


**Figure 3.** Crystal structure of compound **3** bound to DLK. Ligand carbon atoms are colored green to distinguish it from the surrounding ligand-proximal side chains (brown) and ordered water molecules (cyan). Hydrogen-bond interactions (dashed lines) between the ligand and the DLK hinge region anchor the core scaffold pyridine and pyrazole ring systems, presenting the trifluoromethyl moiety near the gatekeeper Met190. The malleable DLK P-loop curls around the ligand isopropyl with a notable inward orientation of Gln136 at its tip. The foreground piperidine moiety clears the lower hinge segment and extends from the binding cavity toward greater solvent exposure.

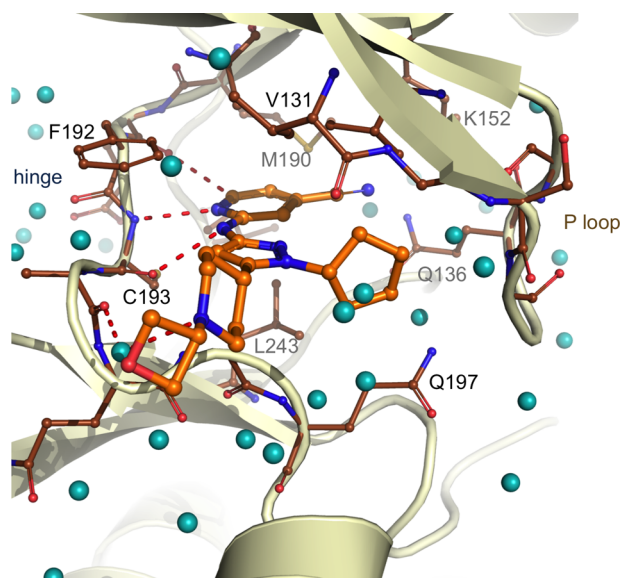


**Figure 4.** Crystal structure of compound **11** bound to DLK. Representations are similar to Figure 3, here with ligand carbon atoms colored orange. The core scaffold maintains key hydrogen-bond interactions with the hinge segment, while the back region cyano group and the forward cyclopentyl moiety engage the P-loop. The solvent-exposed portion of the ligand extends an oxetane beyond the piperidine.

aligned structural features that are achieved around the pyridine to pyrazole core scaffold hopping design.

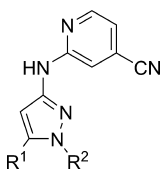
From the SAR examined, inhibitor **11** offered the best balance for potency, in vitro metabolic stability and desirable efflux properties. Broad profiling in an Life Technologies panel

of 58 representative kinases revealed good overall selectivity with no off-target kinases displaying >70% inhibition @ 1  $\mu$ M (Figure 6). We then further evaluated **11** against other members of the mixed lineage kinase family and kinases within the JNK pathway through a 10-point dose–response analysis in an enzymatic assay. Good selectivity was observed against all JNK isoforms (Table 5, JNK1  $IC_{50}$  = 1.04  $\mu$ M, JNK2  $IC_{50}$  = 5  $\mu$ M, and JNK3  $IC_{50}$  = 2.1  $\mu$ M), and no activity was observed at the top concentrations tested for MKK4/7 and MLKs (Table 5). To confirm that inhibitor **11** sufficiently inhibited DLK activity to elicit protection of neurons from degeneration, it was tested in a high content neurodegeneration assay where it protected neurons with an  $EC_{50}$  of  $2.15 \pm 0.56$   $\mu$ M.<sup>28</sup> As expected, the  $EC_{50}$  required for protection of neurons was higher than that observed in the p-JNK assay, as near complete inhibition of DLK activity is required to elicit neuroprotection in this setup.<sup>10</sup> This is consistent with the ratio of the cell-based activity/neuroprotection  $EC_{50}$  observed in the same assay for JNK published inhibitor SP600125.<sup>28</sup> To confirm that the neuroprotection observed with **11** was a result selective DLK inhibition rather than inhibition of downstream kinases, levels of p-MKK4, p-MKK7, p-JNK, and p-c-Jun were examined following overexpression of DLK or constitutively active JNK construct (CA-JNK) to induce pathway activity.<sup>29</sup> Overexpression of DLK resulted in increases in the phosphorylation of MKK4, MKK7, JNK, and c-Jun, while CA-JNK only induced JNK and c-Jun, consistent with previous studies.<sup>5,29</sup> The addition of **11** reduced phosphorylation of all of these signaling components following DLK overexpression, indicating that inhibition of pathway activity indeed occurred at the level of DLK rather than a downstream signaling component (Figure 7). This was further supported by the lack of pathway inhibition observed with **11** following overexpression of CA-JNK (Figure 7). Levels of total JNK were not affected by compound treatment. Taken together, the overall properties of inhibitor **11** were suitable to warrant progression of this molecule for in vivo assessment.

Inhibitor **11** exhibited moderate pharmacokinetic properties and good brain penetration in rat ( $CL_p$  = 34 mL/min/kg,  $V_{dss}$  = 4.4 L/kg,  $t_{1/2}$  = 1.7 h,  $F$  = 58%,  $B_u/P_u$  = 0.354). Although having similar total plasma clearance to inhibitor **2** (Table 6), inhibitor **11** afforded significantly improved free clearance ( $CL_u$  = 327 mL/min/kg). Additionally, **11** had sufficient oral exposure in mouse (50 mpk  $C_{max}$  = 5.9  $\mu$ M,  $T_{max}$  = 0.25 h,  $AUC_{0-6h}$  = 15.8 h\* $\mu$ M, free brain @ 6 h = 0.050  $\mu$ M) to warrant examination in a PK/PD model based on the optic nerve crush injury in mice. As previously described, this model mimics the neuronal degeneration that occurs in glaucoma or optic neuropathy.<sup>9,10</sup> Optic nerve crush robustly induces phosphorylation of c-Jun (p-c-Jun) in a DLK-/JNK-dependent fashion and could thus be used as a pharmacodynamic readout of DLK inhibition in vivo.<sup>9,10,13</sup> Animals were dosed orally with either inhibitor **11** or vehicle control 30 min prior to nerve crush injury, and levels of p-c-Jun in retina were measured 6 h after injury. As predicted by the levels of free compound in brain, treatment with 75 mg/kg inhibitor **11** resulted in a reduction of p-c-Jun present in retina comparable to inhibitor **2** (Figure 8).<sup>13</sup>

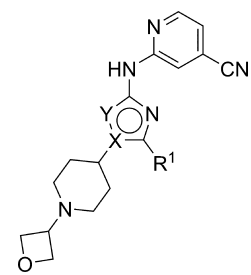
## CHEMISTRY

The syntheses of **3–6**, **9**, **10**, **15**, and **16** were carried out as outlined in Scheme 1. The synthesis of *tert*-butyl 4-(3-amino-1-isopropyl-1H-pyrazol-5-yl)piperidine-1-carboxylate (**38**) com-

Table 3. Pyrazole N1-Substituent SAR<sup>a</sup>


Compound	R <sup>1</sup>	R <sup>2</sup>	K <sub>i</sub> (μM)	pJNK IC <sub>50</sub> (μM)	MDR1-MDCK BA/AB (AB) <sup>b</sup>	LM CL <sub>hep</sub> <sup>c</sup> (mL min <sup>-1</sup> kg <sup>-1</sup> ) H/R/M <sup>d</sup>	ClogP	tPSA	LipE
11			0.042	0.536	1.4 (8.8)	12/33/75	3.7	78	3.7
12			0.048	0.721	5.8 (4.2)	15/-/69	3.8	79	3.5
13			0.378	-	7.6 (1.9)	12/22/56	2.3	88	4.1
14			0.593	-	15 (1.7)	-/-/-	2.7	88	3.5
15			0.133	1.4	-(1.8)	12/37/74	3.5	79	3.4
16			0.048	0.459	3.3 (4.9)	9/40/80	2.9	79	4.4
17			0.025	0.632	3.7 (5.6)	15/42/80	3.3	79	4.3
18			0.054	0.698	1 (2.7)	16/44/82	3.5	75	3.8

<sup>a</sup>Compounds 12, 13, 17, and 18 were tested as racemates, and also subsequent separation into the chirally pure enantiomers showed no additional benefit (not reported). All assay results represent the geometric mean of a minimum of two determinations, and these assays generally produced results within 3-fold of the reported mean. <sup>b</sup>MDCK-MDR1 human P-gp transfected cell line. Basolateral-to-apical/apical-to-basolateral. Units = × 10<sup>-6</sup> cm s<sup>-1</sup>. <sup>c</sup>Liver microsome-predicted hepatic clearance. <sup>d</sup>H/R/M = human/rat/mouse. <sup>e</sup>LipE = -log K<sub>i</sub> - clogP.

Table 4. Thiazole and Imidazole Core Examples<sup>a</sup>


Compound	X	Y	R <sup>1</sup>	K <sub>i</sub> (μM)	pJNK IC <sub>50</sub> (μM)	MDR1-MDCK BA/AB (AB) <sup>b</sup>	ClogP	tPSA	LipE <sup>c</sup>
19	C	S		0.569	8.6	0.94 (15.4)	3.3	74	2.9
20	N	CH		>1.6	-	-(-)	3.2	79	<2.6

<sup>a</sup>All assay results represent the geometric mean of a minimum of two determinations, and these assays generally produced results within 3-fold of the reported mean. <sup>b</sup>MDCK-MDR1 human P-gp transfected cell line. Basolateral-to-apical/apical-to-basolateral. <sup>c</sup>LipE = -log K<sub>i</sub> - clogP.

menced with the acylation of acetonitrile anion with commercially available 1-*tert*-butyl 4-methylpiperidine-1,4-dicarboxylate (CH<sub>3</sub>CN, K<sup>t</sup>OBu, THF) to provide β-ketonitrile **25**. Condensation of the β-ketonitrile **25** with hydrazine produced aminopyrazole **29** which subsequently afforded *tert*-

butyl 4-(3-(1,3-dioxoisindolin-2-yl)-1*H*-pyrazol-5-yl)-piperidine-1-carboxylate (**33**) upon treatment with phthalic anhydride. *N*-pyrazole alkylation with 2-iodopropane (Cs<sub>2</sub>CO<sub>3</sub>, DMF), followed by protecting group removal, produced *tert*-butyl 4-(3-amino-1-isopropyl-1*H*-pyrazol-5-yl)piperidine-1-car-

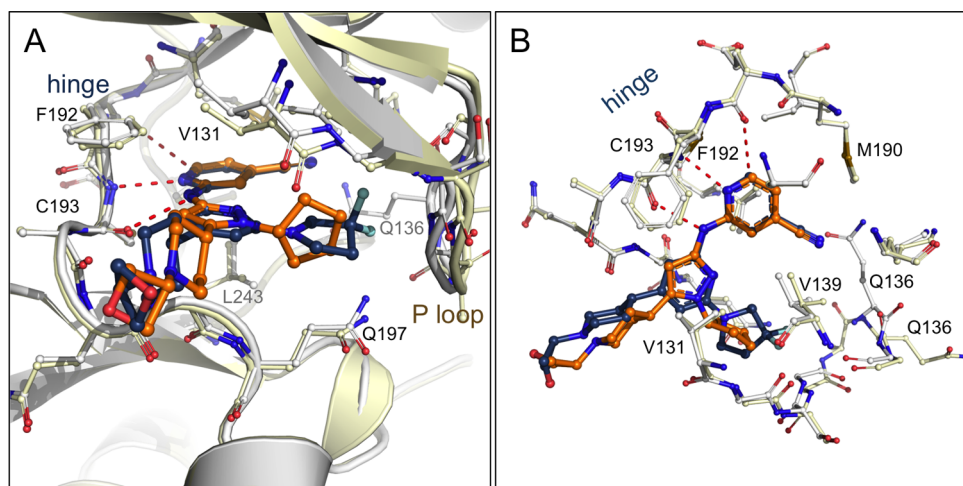


**Figure 5.** Comparison of crystal structure binding modes for compounds **11** and **2** to DLK. The initial lead pyridine-core **2** is shown with carbon atoms in navy blue and DLK protein in ivory, while the scaffold-hop pyrazole-core **11** is depicted with carbon atoms in orange and DLK protein in white. (a) DLK binding mode showing the drape of the P-loop (upper right) around the ligand. The two compounds have an almost exact superposition of the shared back region cyano pyridine moiety. The slightly larger difluoro-pyrrolidine of **2** engages the P-loop to create a slightly outward trajectory (ivory). (b) A cut-away top-down view of the ligand with the DLK hinge at upper left shows the precise cyano-pyridine alignment and conserved hinge interactions of both ligands. The five-membered pyrazole versus six-membered pyridine core ring provides altered vectors, though the outer substituents converge into shared spatial position. The shifted orientation of Gln136 seen at right from its inward ligand-proximal juxtaposition in the compound **11** structure (orange/white) to an outward display in the case of compound **2** binding (navy/ivory) is likely related to the shifted P-loop response from the difluoro-pyrrolidine moiety.

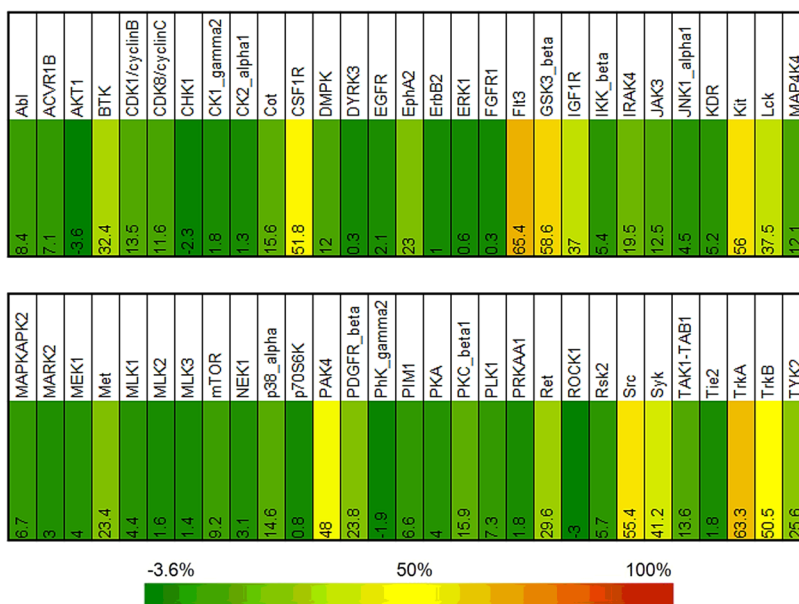


**Figure 6.** Kinase selectivity of compound **11** @ 1uM ( $24 \times$  DLK  $K_i$ ). Values are reported as percent inhibition and determined at Life Technologies. 58 representative kinases were selected from various branches of the kinome tree that were frequent off-targets against a large and diverse panel of internally derived inhibitors. Kinases with  $>50\%$  inhibition are CSF1R ( $IC_{50} = 0.057$  mM), Flt3 ( $IC_{50} = 0.322$  mM), GSK3\_beta ( $IC_{50} = 0.682$  mM), Kit ( $IC_{50} = 0.534$  mM), Src ( $IC_{50} = 1.01$  mM), TrkA ( $IC_{50} = 0.464$  mM), and TrkB ( $IC_{50} = 1.19$  mM). Biochemical  $IC_{50}$  values were determined at Life Technologies.

**Table 5. Kinase Selectivity of Compound **11**<sup>a</sup>**

$K_i$ ( $\mu$ M)	$IC_{50}$ ( $\mu$ M)							
DLK	MKK4	MKK7	JNK1 <sup>b</sup>	JNK2 <sup>b</sup>	JNK3 <sup>b</sup>	MLK1 <sup>b</sup>	MLK2 <sup>b</sup>	MLK3 <sup>b</sup>
0.042	>5	>5	1.04	5	2.1	>10	>10	>10

<sup>a</sup>Biochemical  $IC_{50}$  determination. <sup>b</sup>Biochemical  $IC_{50}$  determination at Life Technologies.

boxylate (**38**). Buchwald–Hartwig reaction of **38** with the required heteroaryl bromides followed by *N*-Boc deprotection

furnished **3–6**. Acylation of compound **4** with acetic anhydride provided acetamide **9**, while reductive amination with oxetan-3-

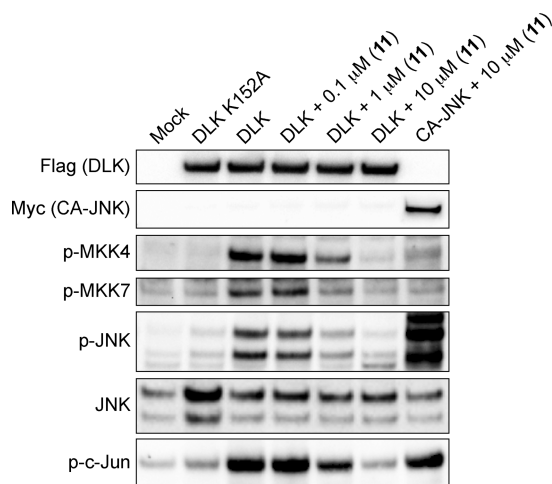


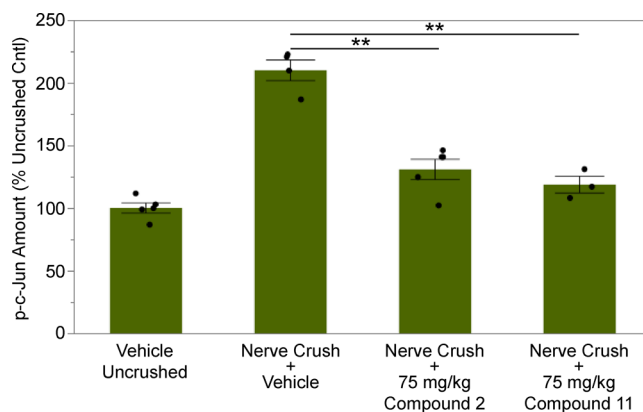
**Figure 7.** Transfection of HEK293 cells with Flag DLK results in increase phosphorylation of MKK4 (p-MKK4), MKK7 (p-MKK7), JNK (p-JNK), and c-Jun (p-c-Jun), while transfection of a kinase dead form of DLK (Flag DLK K152A) does not. Addition of increasing concentrations of compound 11 (0.1, 1, or 10  $\mu$ M) reduces levels p-MKK4, p-MKK7, p-JNK, and p-c-Jun. Levels of total JNK are not affected by addition of compound. Ten  $\mu$ M of compound 11 is not able to reduce p-c-Jun induced by overexpression of a constitutively active JNK (Myc CA-JNK).

**Table 6.** PK Properties of DLK Inhibitors 1, 2, and 11<sup>a</sup>

	1	2	11
Rat <sup>b</sup>			
CL <sub>p</sub> (mL min <sup>-1</sup> kg <sup>-1</sup> )	45	30	34
CL <sub>u</sub> (mL min <sup>-1</sup> kg <sup>-1</sup> ) <sup>c</sup>	45000	2500	327
V <sub>dss</sub> (L kg <sup>-1</sup> )	3.8	3.7	4.4
t <sub>1/2</sub> (h)	1.2	1.8	1.7
F (%)	16	63	58
B <sub>u</sub> /P <sub>u</sub> <sup>d</sup>	1.3	0.7	0.35
Free AUC/dose (h·kg·L <sup>-1</sup> )	0.00006	0.004	0.03
Mouse (PO 50 mg kg <sup>-1</sup> ) <sup>e</sup>			
C <sub>max</sub> ( $\mu$ M)		4.38	5.9
T <sub>max</sub> (h)		0.8	0.25
AUC <sub>0-6h</sub> (h· $\mu$ M)		12.8	15.8
B <sub>u</sub> ( $\mu$ M) @ 6 h		0.004	0.050

<sup>a</sup>Rat PK properties of compounds 1, 2, and 11. Mouse 50 mg kg<sup>-1</sup> PO PK properties of compounds 2 and 11. <sup>b</sup>Compounds were dosed iv (0.4 or 1 mg kg<sup>-1</sup>) as a 60% PEG solution and po (1 or 5 mg kg<sup>-1</sup>) as an aqueous suspension with 1% methylcellulose. <sup>c</sup>CL<sub>u</sub> = CL/f<sub>u</sub> (f<sub>u</sub> = fraction unbound in plasma). <sup>d</sup>Unbound brain/unbound plasma AUC ratio (unless noted otherwise). <sup>e</sup>Compounds dosed po (50 mg kg<sup>-1</sup>) as an aqueous suspension with 1% methylcellulose.

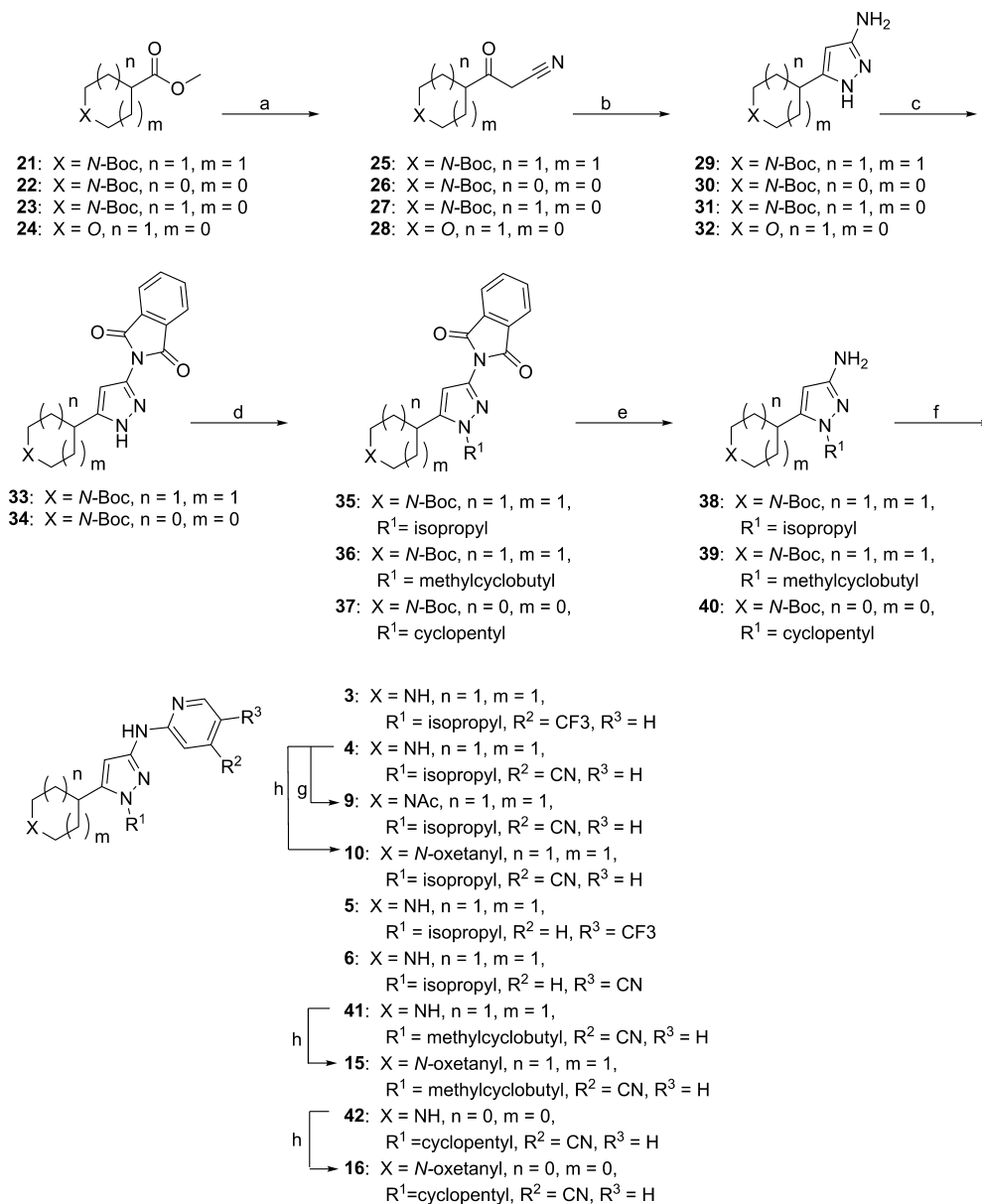
one provided *N*-oxetane 10. Similar to the synthesis of 10, compound 15 was obtained by alkylation of 33 with (bromomethyl)cyclobutane. Likewise, compound 16 was made with commercially available 1-*tert*-butyl 3-methyl azetidine-1,3-dicarboxylate (22) with subsequent alkylation of 34 with bromocyclopentane. The preparation of compounds 7, 8, and 11 was performed as shown in Scheme 2. Protection of *tert*-butyl 4-(3-amino-1*H*-pyrazol-5-yl)piperidine-1-carboxylate (29) with 2,5-hexanedione afforded *tert*-butyl 4-(3-(2,5-dimethyl-1*H*-pyrrol-1-yl)-1*H*-pyrazol-5-yl)piperidine-1-carboxylate (43). *N*-pyrazole alkylation with iodocyclopentane followed by 2,5-dimethylpyrrole deprotection (NH<sub>2</sub>OH, KOH, EtOH) yielded *tert*-butyl 4-(3-amino-1-cyclopentyl-1*H*-



**Figure 8.** Compound 11 displays comparable activity to compound 2 in the optic nerve crush model. Levels of p-c-Jun in retinal lysates measured by ELISA following nerve crush and treatment with inhibitor 11 or 2. Values are presented relative to uncrushed vehicle controls, \*\**p* < 0.01. Bars represent the mean and error bars represent SEM. Dots represent data points from individual animals in the study.

pyrazol-5-yl)piperidine-1-carboxylate (45). Buchwald–Hartwig reaction of 45 with 2-bromo-4-(trifluoromethyl)pyridine and 2-bromoisonicotinonitrile provided compounds 7 and 8, respectively, after *N*-Boc deprotection. Oxetane 11 was obtained by reductive amination with oxetan-3-one. The syntheses of 12–14, 17, and 18 were conducted as outlined in Scheme 3. Sandmeyer reaction of *tert*-butyl 4-(3-amino-1*H*-pyrazol-5-yl)piperidine-1-carboxylate (29) resulted in iodopyrazole 46 which was utilized in the syntheses of intermediates 50–52. Hafnium chloride<sup>30</sup> catalyzed conjugate addition of 46 to cyclopent-2-enone followed by fluorination with DAST afforded *tert*-butyl 4-(1-(3,3-difluorocyclopentyl)-3-iodo-1*H*-pyrazol-5-yl)piperidine-1-carboxylate (50). Intermediates 51 and 52 were obtained by the reaction of 46 with tetrahydrofuran-3-yl methanesulfonate and tetrahydro-2*H*-pyran-4-yl methanesulfonate respectively (NaH, DMF). Aminopyrazoles 31 and 32 followed the same procedure as 29 (Scheme 1) with substitution of *tert*-butyl 3-methyl pyrrolidine-1,3-dicarboxylate (23) and methyl tetrahydrofuran-3-carboxylate (24) for 1-*tert*-butyl 4-methylpiperidine-1,4-dicarboxylate, respectively. Subsequent iodination and *N*-pyrazole alkylation with bromocyclopentane yielded intermediates 53 and 54. Modified Goldberg coupling<sup>31–33</sup> of 50–53 with aminoisonicotinonitrile, acid-mediated *N*-Boc deprotection, and reductive amination with oxetan-3-one furnished 12–14 and 17. Compound 18 was obtained via Goldberg coupling of aminoisonicotinonitrile with 54. The preparation of compound 19 was performed as shown in Scheme 4. Starting with commercially available 4-cyclopropylthiazol-2-amine (55) mono *N*-Boc protection (56) followed by chlorination (*N*-chlorosuccinimide) led to intermediate 57. Suzuki–Miyaura cross coupling of 57 with *tert*-butyl 4-(4,4,5,5-tetramethyl-1,3,2-dioxaborolan-2-yl)-5,6-dihydropyridine-1(2*H*)-carboxylate provided alkene 58 which was reduced by hydrogenation to obtain intermediate 59. Removal of the *tert*-butoxycarbonyl protective groups provided 60, and subsequent reductive amination with oxetan-3-one provided the *N*-oxetanylpiperidine 61. Compound 19 was attained via Buchwald–Hartwig coupling of chloroisonicotinonitrile with 61. The synthesis of compound 20 was performed as highlighted in Scheme 5. Iodination of commercially available 2-cyclopentylimidazole (62) followed by regioselective reduction gave monoiodoimidazole 64.<sup>34</sup> Inter-



Scheme 1<sup>a</sup>

<sup>a</sup>Reagents and conditions: (a) CH<sub>3</sub>CN, K<sup>t</sup>OBu, THF, 23 °C, 1 h; (b) hydrazine monohydrate, *i*-PrOH, 80 °C, 18 h; (c) phthalic anhydride, 1,4-dioxane, 90 °C, 18 h; (d) R-I or R-Br, Cs<sub>2</sub>CO<sub>3</sub>, DMF, or DMA, 50–110 °C, 3 h–16 h; (e) hydrazine hydrate, MeOH, 23 °C, 30 min; (f) i. R-Br, Pd<sub>2</sub>(dba)<sub>3</sub>, Xantphos, *t*-BuONa, 1,4-dioxane, 80 °C, 3 h; ii. HCl in 1,4-dioxane, MeOH, 23 °C, 16 h; (g) acetic anhydride, TEA, DMF, 40 °C, 16 h, 58%; (h) 3-oxetanone, Na(OAc)<sub>3</sub>BH, DCM, 23 °C, 1 h.

mediate **65** was obtained by reaction of **64** with *tert*-butyl 4-((methylsulfonyl)oxy)piperidine-1-carboxylate (NaH, DMF). Goldberg coupling of **65** with aminoisonicotinonitrile followed by acid-mediated *N*-Boc deprotection and final reductive amination with oxetan-3-one procured analog **20**.

## CONCLUSIONS

The scaffold-hopping approach described herein, facilitated by our determination of the first DLK structures, provided a complementary method to optimize compound **1** by improving physicochemical properties. Although less potent than the inhibitor **2**,<sup>13</sup> inhibitor **11** possessed improved free drug exposure; thus providing inhibitors with equivalent *in vivo* inhibition of the DLK/JNK pathway, but with increased

potential for further optimization as a small molecule therapeutic.

## METHODS

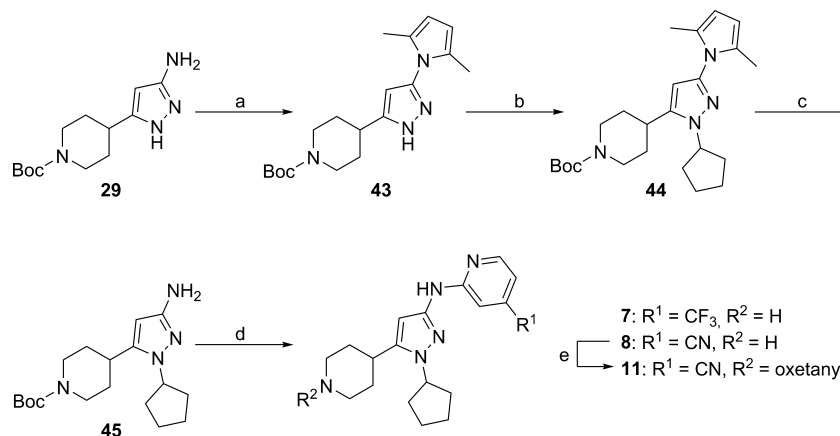
**DLK Biochemical Assay.** The biochemical assay was performed as previously described.<sup>35</sup>

**p-JNK Cell Assay.** The p-JNK cell assay for generation of IC<sub>50</sub> values was performed as previously described.<sup>13</sup>

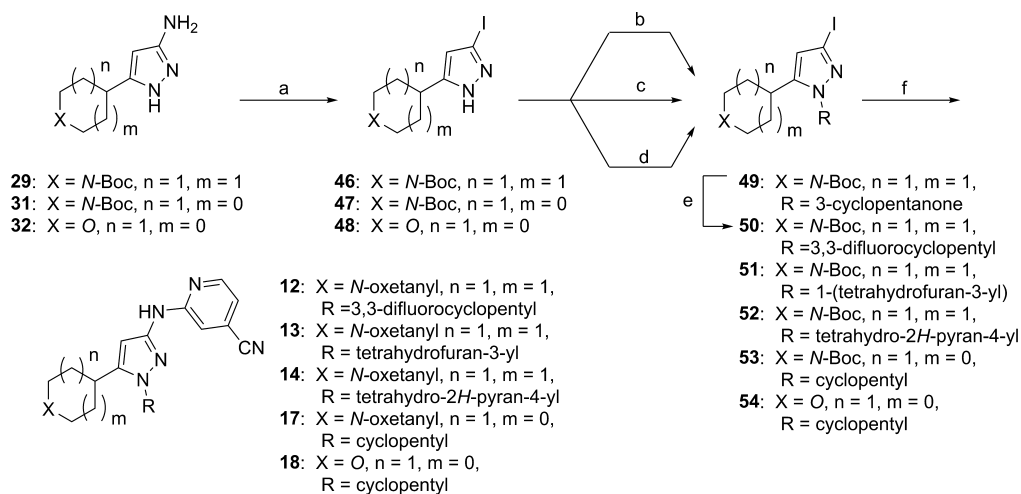
**DLK and CA-JNK Transfection Cell Assays.** DLK and CA-JNK transfection assays to assess pathway selectivity were performed as described.<sup>5</sup> Cells were treated with compound for 5 h, and the transfection was performed 24 h prior to compound treatment.

**In Vitro Axon Degeneration Cell Assay.** Assay was conducted as previously described.<sup>36</sup>

**MKK4 and MKK7 Biochemical Assays.** MKK4 enzymatic reaction was initiated by combining 30 nM MKK4 with 100 μM

Scheme 2<sup>a</sup>

<sup>a</sup>Reagents and conditions: (a) 2,5-hexadione, MgSO<sub>4</sub>, toluene, 40 °C, 16 h, 97% crude yield; (b) iodocyclopentane, Cs<sub>2</sub>CO<sub>3</sub>, DMF, 50 °C, 16 h, 69% yield; (c) hydroxylamine, KOH, EtOH, 80 °C, 16 h, 34% yield; (d) *i.* R-Br, Pd<sub>2</sub>(dba)<sub>3</sub>, Xantphos, *t*-BuONa, 1,4-dioxane, 80 °C, 3h; *ii.* HCl in 1,4-dioxane, MeOH, 23 °C, 16 h; (e) 3-oxetanone, Na(OAc)<sub>3</sub>BH, DCM, 23 °C, 1 h.

Scheme 3<sup>a</sup>

<sup>a</sup>Reagents and conditions: (a) NaI, NaNO<sub>2</sub>, *p*-toluenesulfonic acid monohydrate, ACN, H<sub>2</sub>O, 0 °C, 1 h; (b) cyclopent-2-eneone, hafnium tetrachloride, DCM, 23 °C, 12 h, 100% crude yield; (c) R-OSO<sub>2</sub>Me, NaH, DMF, 60–90 °C, 2–4 h; (d) bromocyclopentane, Cs<sub>2</sub>CO<sub>3</sub> or K<sub>2</sub>CO<sub>3</sub>, DMF, 50–80 °C, 2–3 h; (e) DAST, DCM, 23 °C, 12 h, 20% yield; (f) *i.* 2-aminoisonicotinonitrile, CuI, N<sup>1</sup>,N<sup>2</sup>-dimethylcyclohexane-1,2-diamine, K<sub>3</sub>PO<sub>4</sub>, DMF, 160 °C microwave, 1 h; *ii.* TFA, DCM, 23 °C, 3 h; *iii.* 3-oxetanone, Na(OAc)<sub>3</sub>BH, DCM, 23–60 °C, 1 h.

peptide substrate (KFMMTPpYVVTR), 5  $\mu$ M ATP, and 3.3 nM fluorescence labeled phospho-peptide probe (MpTPpYV) in buffer containing 50 mM HEPES pH 7.5 0.1% Pluronic F-127, 5 mM MgCl<sub>2</sub> 10 mM DTT, 6.25 mM NaCl, 0.1 mM EGTA, and 0.01% BSA. The reaction mixture was incubated at 23 °C for 1 h before the addition of stop mixture (50 mM HEPES pH 7.5 0.1% Pluronic F-127, 6.25 mM NaCl 0.1 mM EGTA, 22.5 mM EDTA, 0.01% BSA and P-SAPK/JNK (T183/Y185) (81E11) Rabbit mAb in 1:1000 dilution). The fluorescence polarization (FP) of the competitive phospho-peptide probe in the final mixture was detected at excitation wavelength of 633 nm and emission wavelength of 670 nm using FCS+ Insight reader (Evotec AG, Germany). The enzymatic activity in the presence of inhibitor was normalized against the signal of positive control. MKK7 reaction was carried out with 100  $\mu$ M peptide substrate (KFMMpTPYVVTR) and 30  $\mu$ M ATP under the same reaction condition.

**In Vitro Transporter Assays.** The in vitro transporter assays were performed as previously described.<sup>13</sup>

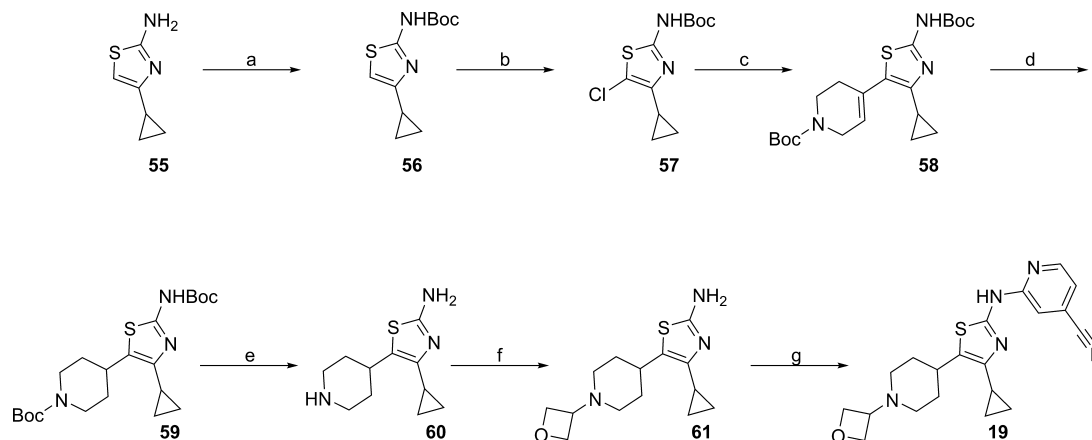
**Life Technologies Kinase Assays.** Compound **11** was tested in Life Technologies' SelectScreen (Madison, WI) against 58 representative kinases at a concentration of 1  $\mu$ M, which is 24-fold greater than

the  $K_i$  for the compound against human recombinant DLK in the DLK enzyme assay. The kinase assays were carried out using Z'-LYTE Technology (Life Technologies, Madison WI) which measured labeled peptide phosphorylation via fluorescence resonance energy transfer (FRET) following protocols developed and performed by Life Technologies.<sup>37</sup>

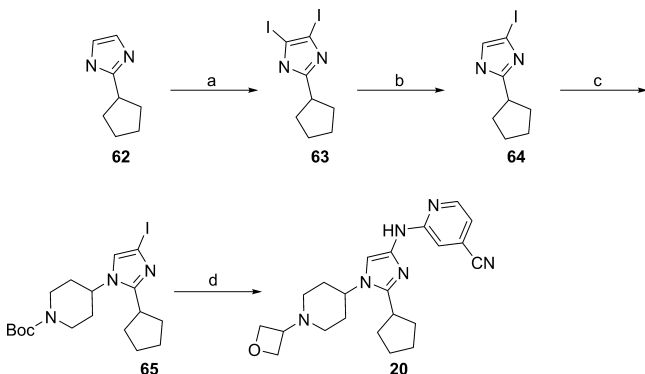
**Animal Models.** All experiments with mice were performed under animal protocols approved by the Animal Care and Use Committee at Genentech and adhere to ACS Ethical Guidelines for animal studies. For all in vivo studies, C57/BL6 mice were dosed with compound **11** orally as an MCT suspension. Optic nerve crush studies were conducted as described,<sup>9</sup> except p-c-Jun was measured at 6 h by MSD ELISA (MesoScale Discovery).

## ■ EXPERIMENTAL SECTION

**General.** All commercially available reagents and solvents were used as received. Reactions using air- or moisture-sensitive reagents were performed under an atmosphere of nitrogen using freshly opened EMD DriSolv solvents. Reaction progress was monitored by TLC and/or LCMS. Flash chromatography was performed with Isco

Scheme 4<sup>a</sup>

<sup>a</sup>Reagents and conditions: (a) di-*tert*-butyl dicarbonate, 80 °C, 5 h, 74% yield; (b) *N*-chlorosuccinimide, 0 °C, 2 h, 85% yield; (c) *tert*-butyl 4-(4,4,5,5-tetramethyl-1,3,2-dioxaborolan-2-yl)-5,6-dihydropyridine-1(2H)-carboxylate, Pd<sub>2</sub>(dba)<sub>3</sub>, Xantphos, 1,4-dioxane, H<sub>2</sub>O, 100 °C, 4 h, 47% yield; (d) H<sub>2</sub>, MeOH, 10% Pd/C, 55 psi, 98% crude yield; (e) TFA, DCM, 30 °C, 4 h, 100% crude yield; (f) 3-oxetanone, Na(OAc)<sub>3</sub>BH, DCM, 23 °C, 1 h, 62% crude yield; (g) 2-chloroisonicotinonitrile, Pd(*t*-Bu<sub>3</sub>P)<sub>2</sub>, K<sub>3</sub>PO<sub>4</sub>, 1,4-dioxane, 100 °C, 3 h, 5% yield.

Scheme 5<sup>a</sup>

<sup>a</sup>Reagents and conditions: (a) I<sub>2</sub>, aq NaOH, 50 °C, 6 h, 35% yield; (b) Na<sub>2</sub>SO<sub>3</sub>, EtOH, reflux, 10 h, 74% yield; (c) *tert*-butyl 4-((methylsulfonyl)oxy)piperidine-1-carboxylate, NaH, DMF, 100 °C, 8 h, 8% yield; (d) *i.* 2-aminoisonicotinonitrile, CuI, N<sup>1</sup>,N<sup>2</sup>-dimethylcyclohexane-1,2-diamine, K<sub>3</sub>PO<sub>4</sub>, DMF, 160 °C microwave, 1 h; *ii.* HCl in 1,4-dioxane, MeOH, 23 °C, 16 h; *iii.* 3-oxetanone, Na(OAc)<sub>3</sub>BH, DCM, 23 °C, 1 h, 8% yield.

CombiFlash Companion systems using prepacked silica gel columns (40–60 μm particle size RediSep or 20–40 μm spherical silica gel RediSep Gold columns or similar columns from other vendors). Preparative reverse-phase HPLC purifications were performed on a Varian Prostar instrument, using a Phenomenex Gemini-NX C-18 (3 × 5 cm; 5 μm) stationary phase, with 0.1% aqueous formic acid/acetonitrile or 0.1% aqueous ammonium hydroxide/acetonitrile gradients as the mobile phase (typically 5–85% acetonitrile over 10 min) with a flow rate of 60 mL/min. NMR spectra were measured on Bruker 300, 400, or 500 MHz spectrometers, and chemical shifts were reported in ppm downfield from TMS using residual nondeuterated solvent as internal standards (CHCl<sub>3</sub>, 7.26 ppm; DMSO, 2.50 ppm; MeOH, 3.31 ppm). The following abbreviations are used: br = broad signal, s = singlet, d = doublet, dd = doublet of doublets, t = triplet, q = quartet, m = multiplet. The purity of final compounds was verified by HPLC to be >95% in all cases using either of the following methods: (1) Agilent 1200 instrument with an Agilent SB C-18 (2.1 × 30 mm; 1.8 μm particle size) stationary phase, and a gradient of water/acetonitrile (5–95% over 10 min; 0.05% TFA in both phases) at a flow rate of 0.4 mL/min. Quantification of target and impurities was done by UV detection at 254 nm; (2) Shimadzu LC-2010A/2020A

instrument with an Ultimate C-18 (3.0 × 50 mm; 3 μm particle size) stationary phase, and a gradient of water/acetonitrile (10–80% over 6 min then 80% over 2 min; 0.05% TFA in both phases) at a flow rate of 1.2 mL/min and oven temperature of 40 °C. Quantification of target and impurities was done by UV detection at 254 nm.

*N*-(1-Isopropyl-5-(piperidin-4-yl)-1H-pyrazol-3-yl)-4-(trifluoromethyl)pyridin-2-amine (3). A mixture of 38 (0.10 g, 0.33 mmol), 2-bromo-4-(trifluoromethyl)pyridine (59 mg, 0.26 mmol), sodium *tert*-butoxide (32 mg, 0.33 mmol), 4,5-bis-(diphenylphosphino)-9,9-dimethylxanthene (16 mg, 0.017 mmol), and tris(dibenzylideneacetone)dipalladium(0) (15 mg, 0.026 mmol) in 1,4-dioxane (10 mL) was heated at 80 °C for 16 h. The reaction mixture was filtered and diluted with water (15 mL). The resulting solution was extracted with ethyl acetate (2 × 15 mL). The collected organic was dried over anhydrous sodium sulfate, filtered, and concentrated under reduced pressure. The residue was dissolved in methanol (2 mL), and a 4.0 M solution of hydrogen chloride in 1,4-dioxane (0.5 mL, 2 mmol) was added. After 16 h, the mixture was concentrated under reduced pressure and purified by preparative reverse-phase HPLC to afford the title compound as an off-white solid (64 mg, 55% yield). LCMS: *m/z* = 354.1 [M + H]<sup>+</sup>; <sup>1</sup>H NMR (400 MHz, DMSO-*d*<sub>6</sub>) δ 9.76 (s, 1H), 8.46–8.24 (m, 2H), 7.61 (s, 1H), 7.00–6.87 (m, 1H), 6.12 (s, 1H), 4.62–4.43 (m, 1H), 3.17 (d, *J* = 12.4 Hz, 2H), 3.01–2.87 (m, 1H), 2.87–2.73 (m, 2H), 1.86 (d, *J* = 13.1 Hz, 2H), 1.70–1.53 (m, 2H), 1.37 (d, *J* = 6.4 Hz, 6H).

2-(1-Isopropyl-5-(piperidin-4-yl)-1H-pyrazol-3-ylamino)-isonicotinonitrile (4). A mixture of 38 (821 mg, 2.00 mmol), 2-bromoisonicotinonitrile (403 mg, 2.20 mmol), 4,5-bis-(diphenylphosphino)-9,9-dimethylxanthene (89.0 mg, 0.150 mmol), tris(dibenzylideneacetone)dipalladium(0) (92.0 mg, 0.100 mmol), and sodium *tert*-butoxide (269 mg, 2.80 mmol) in 1,4-dioxane (8 mL) was heated at 80 °C for 16 h. The reaction mixture was filtered and diluted with water (15 mL). The resulting solution was extracted with ethyl acetate (2 × 30 mL). The collected organic was dried over anhydrous sodium sulfate, filtered, and concentrated under reduced pressure. The residue was dissolved in dichloromethane (15 mL), and a 4.0 M solution of hydrogen chloride in 1,4-dioxane (0.80 mL, 3.20 mmol) was added. After 16 h at 23 °C, the reaction mixture was concentrated under reduced pressure to afford crude title compound (597 mg, 66% crude yield). A portion of the crude (102 mg, 0.330 mmol) was purified by preparative reverse-phase HPLC to afford the title compound as an off-white solid (22 mg, 21%). LCMS: *m/z* = 311.1 [M + H]<sup>+</sup>; <sup>1</sup>H NMR (400 MHz, DMSO-*d*<sub>6</sub>) δ 9.75 (s, 1H), 8.31 (d, *J* = 5.1 Hz, 1H), 7.50 (s, 1H), 7.01 (d, *J* = 5.1 Hz, 1H), 6.13 (s, 1H), 4.58–4.39 (m, 1H), 3.02–2.91 (m, 2H), 2.84–2.69 (m, 1H), 2.69–

2.54 (m, 1H), 2.07 (s, 1H), 1.79–1.67 (m, 3H), 1.51–1.41 (m, 2H), 1.36 (d,  $J = 6.4$  Hz, 6H).

*N*-(1-Isopropyl-5-(piperidin-4-yl)-1H-pyrazol-3-yl)-5-(trifluoromethyl)pyridin-2-amine (**5**). The title compound (17 mg, 15% yield) was prepared in a manner analogous to **3** by substituting 2-bromo-5-(trifluoromethyl)pyridine for 2-bromo-4-(trifluoromethyl)pyridine. LCMS:  $m/z = 354.1$  [ $M + H$ ]<sup>+</sup>; <sup>1</sup>H NMR (400 MHz, DMSO-*d*<sub>6</sub>)  $\delta$  9.90 (s, 1H), 8.44 (s, 1H), 7.86–7.78 (m, 1H), 7.25 (d,  $J = 8.9$  Hz, 1H), 6.21 (s, 1H), 4.55–4.43 (m, 1H), 2.98 (d,  $J = 12.2$  Hz, 2H), 2.82–2.70 (m, 1H), 2.64–2.53 (m, 2H), 2.10 (s, 1H), 1.77–1.68 (m, 2H), 1.51–1.33 (m, 8H).

6-(1-Isopropyl-5-(piperidin-4-yl)-1H-pyrazol-3-ylamino)-nicotinonitrile (**6**). The title compound (29 mg, 28% yield) was prepared in a manner analogous to **3** by substituting 6-bromonicotinonitrile for 2-bromo-4-(trifluoromethyl)pyridine. LCMS:  $m/z = 311.3$  [ $M + H$ ]<sup>+</sup>; <sup>1</sup>H NMR (400 MHz, DMSO-*d*<sub>6</sub>)  $\delta$  10.11 (s, 1H), 8.53 (s, 1H), 7.87 (dd,  $J = 8.8, 2.3$  Hz, 1H), 7.20 (s, 1H), 6.21 (s, 1H), 4.50 (p,  $J = 6.4$  Hz, 1H), 3.02–2.93 (m, 2H), 2.82–2.71 (m, 1H), 2.58 (t,  $J = 12.1$  Hz, 2H), 2.05 (s, 1H), 1.77–1.68 (m, 2H), 1.50–1.38 (m, 2H), 1.36 (d,  $J = 6.4$  Hz, 6H).

*N*-(1-Cyclopentyl-5-(piperidin-4-yl)-1H-pyrazol-3-yl)-4-(trifluoromethyl)pyridin-2-amine (**7**). The title compound (5.4 mg, 7% yield) was prepared in a manner analogous to **3** by substituting *tert*-butyl 4-(3-amino-1-cyclopentyl-1H-pyrazol-5-yl)piperidine-1-carboxylate for *tert*-butyl 4-(3-amino-1-isopropyl-1H-pyrazol-5-yl)piperidine-1-carboxylate. LCMS:  $m/z = 380.2$  [ $M + H$ ]<sup>+</sup>; <sup>1</sup>H NMR (400 MHz, DMSO-*d*<sub>6</sub>)  $\delta$  9.69 (s, 1H), 8.34 (d,  $J = 5.3$  Hz, 1H), 7.76 (s, 1H), 6.94 (dd,  $J = 5.2, 1.6$  Hz, 1H), 6.02 (s, 1H), 4.73–4.65 (m, 1H), 3.08–2.92 (m, 2H), 2.86–2.77 (m, 1H), 2.70–2.56 (m, 3H), 2.09–1.97 (m, 2H), 1.93–1.82 (m, 4H), 1.81–1.69 (m, 2H), 1.70–1.61 (m, 2H), 1.51–1.32 (m, 2H).

2-((1-Cyclopentyl-5-(piperidin-4-yl)-1H-pyrazol-3-yl)amino)-isonicotinonitrile (**8**). A mixture of **45** (1.20 g, 0.350 mmol), 2-bromoisonicotinonitrile (175 mg, 0.385 mmol), 4,5-bis-(diphenylphosphino)-9,9-dimethylxanthene (16 mg, 0.026 mmol), tris(dibenzylideneacetone)dipalladium(0) (16 mg, 0.018 mmol) and sodium *tert*-butoxide (47 mg, 0.49 mmol) in 1,4-dioxane (12 mL) was stirred at 80 °C for 16 h. The reaction mixture was filtered and diluted with water (15 mL). The resulting solution was extracted with ethyl acetate (2 × 30 mL). The collected organic was dried over anhydrous sodium sulfate, filtered, and concentrated under reduced pressure. The residue was dissolved in dichloromethane (15 mL), and a 4 M solution of hydrogen chloride 1,4-dioxane (0.80 mL, 3.2 mmol) was added at 23 °C. After 16 h, the reaction mixture was concentrated under reduced pressure, and a portion of the crude product (117 mg, 0.35 mmol) was purified by preparative reverse-phase HPLC to afford the title compound as an off-white solid (54 mg, 46%). LCMS:  $m/z = 337.2$  [ $M + H$ ]<sup>+</sup>; <sup>1</sup>H NMR (400 MHz, DMSO-*d*<sub>6</sub>)  $\delta$  9.80 (s, 1H), 8.32 (d,  $J = 5.2$  Hz, 1H), 7.55 (s, 1H), 7.03 (d,  $J = 5.2$  Hz, 1H), 6.15 (s, 1H), 4.81–4.59 (m, 1H), 3.08 (t,  $J = 11.9, 3.8$  Hz, 1H), 2.97 (t,  $J = 12.9, 2.8$  Hz, 2H), 2.05–1.83 (m, 10H), 1.79–1.59 (m, 5H).

2-(5-(1-Acetylpiperidin-4-yl)-1-isopropyl-1H-pyrazol-3-ylamino)-isonicotinonitrile (**9**). A mixture of **4** (109 mg, 0.350 mmol), acetic anhydride (41.0 mg, 0.385 mmol), and triethylamine (0.148 mL, 1.05 mmol) in *N,N*-dimethylformamide (1.40 mL) was stirred at 40 °C for 16 h. The mixture was concentrated under reduced pressure and purified by preparative reverse-phase HPLC to afford the title compound as a white solid (71 mg, 58%). LCMS:  $m/z = 353.1$  [ $M + H$ ]<sup>+</sup>; <sup>1</sup>H NMR (400 MHz, DMSO-*d*<sub>6</sub>)  $\delta$  9.83 (s, 1H), 8.31 (d,  $J = 5.2$  Hz, 1H), 7.48 (s, 1H), 7.02 (d,  $J = 5.1$  Hz, 1H), 6.16 (s, 1H), 4.55 (p,  $J = 6.4$  Hz, 1H), 4.51–4.44 (m, 1H), 3.93–3.85 (m, 1H), 3.22–3.10 (m, 1H), 3.05–2.92 (m, 1H), 2.68–2.57 (m, 1H), 2.03 (s, 3H), 1.84 (s, 2H), 1.60–1.46 (m, 1H), 1.38 (d,  $J = 6.5$  Hz, 6H), 1.35–1.27 (m, 1H).

2-(1-Isopropyl-5-(1-(oxetan-3-yl)piperidin-4-yl)-1H-pyrazol-3-ylamino)isonicotinonitrile (**10**). A mixture of **4** (109 mg, 0.350 mmol) and oxetan-3-one (50.0 mg, 0.70 mmol) in dichloromethane (1.75 mL) was stirred at 23 °C for 15 min. Sodium triacetoxyborohydride (234 mg, 1.05 mmol) was added, and the mixture was stirred at 23 °C for 1 h. The reaction mixture was partitioned between dichloro-

methane (15 mL) and saturated aqueous ammonium chloride solution (15 mL). The organic was separated, and the aqueous layer was further extracted with dichloromethane (2 × 5 mL). The collected organic was dried over anhydrous sodium sulfate, filtered, and concentrated under reduced pressure. Purification by preparative reverse-phase HPLC afforded the title compound as a white solid (82 mg, 64%). LCMS:  $m/z = 367.2$  [ $M + H$ ]<sup>+</sup>; <sup>1</sup>H NMR (400 MHz, DMSO-*d*<sub>6</sub>)  $\delta$  9.76 (s, 1H), 8.32 (d,  $J = 5.1$  Hz, 1H), 7.51 (s, 1H), 7.05–6.98 (m, 1H), 6.16 (s, 1H), 4.58–4.40 (m, 5H), 3.47–3.35 (m, 1H), 2.82–2.65 (m, 3H), 1.95–1.74 (m, 4H), 1.66–1.51 (m, 2H), 1.36 (d,  $J = 6.4$  Hz, 6H).

2-((1-Cyclopentyl-5-(1-(oxetan-3-yl)piperidin-4-yl)-1H-pyrazol-3-ylamino)isonicotinonitrile (**11**). A mixture of **8** (236 mg, 0.600 mmol) and oxetan-3-one (87.0 mg, 1.20 mmol) in dichloromethane (5 mL) was stirred at 23 °C for 15 min. Sodium triacetoxyborohydride (381 mg, 1.80 mmol) was added, and the mixture was stirred at 23 °C for an additional 1 h. The reaction mixture was partitioned between dichloromethane (15 mL) and saturated aqueous ammonium chloride solution (15 mL). The organic was separated, and the aqueous layer was further extracted with dichloromethane (2 × 5 mL). The collected organic was dried over anhydrous sodium sulfate, filtered, and concentrated under reduced pressure. Purification by preparative reverse-phase HPLC afforded the title compound as a white solid (142 mg, 60%). <sup>1</sup>H NMR (500 MHz, DMSO-*d*<sub>6</sub>)  $\delta$  9.79 (s, 1H), 8.33 (d,  $J = 5.1$  Hz, 1H), 7.58 (zs, 1H), 7.03 (dd,  $J = 5.1, 1.4$  Hz, 1H), 6.14 (s, 1H), 4.69 (m, 1H), 4.55 (dd,  $J = 6.3, 6.3$  Hz, 2H), 4.44 (dd,  $J = 6.3, 6.3$  Hz, 2H), 3.40 (p,  $J = 6.3$  Hz, 1H), 2.80–2.70 (m, 3H), 2.05–1.95 (m, 2H), 1.93–1.80 (m, 8H), 1.67–1.53 (m, 4H); <sup>13</sup>C NMR (126 MHz, DMSO-*d*<sub>6</sub>)  $\delta$  155.64, 149.93, 147.90, 147.31, 120.35, 117.97, 114.42, 111.87, 92.78, 75.20, 59.13, 57.77, 49.88, 33.10, 32.63, 32.06, 25.04; HRMS (ESI)  $m/z$ : [ $M + H$ ]<sup>+</sup> Calcd for C<sub>22</sub>H<sub>29</sub>N<sub>6</sub>O 393.2397; Found: 393.2397.

2-(1-(3,3-Difluorocyclopentyl)-5-(1-(oxetan-3-yl)piperidin-4-yl)-1H-pyrazol-3-ylamino)isonicotinonitrile (**12**). To a solution of **50** (0.40 g, 0.83 mmol) in *N,N*-dimethylformamide (4 mL) was added 2-aminoisonicotinonitrile (198 mg, 1.66 mmol), *N*<sup>1</sup>,*N*<sup>2</sup>-dimethylcyclohexane-1,2-diamine (24 mg, 0.17 mmol), potassium phosphate (529 mg, 2.49 mmol), and copper iodide (32 mg, 0.17 mmol) and purged with nitrogen. The resulting solution was heated at 160 °C under microwave irradiation for 1 h. The mixture was diluted with ethyl acetate (20 mL) and filtered. The filtrate was extracted with ethyl acetate (3 × 20 mL). The collected organic was washed with saturated aqueous sodium chloride solution (20 mL), dried over sodium sulfate, filtered, and concentrated under reduced pressure. Purification by flash column chromatography (3:1 petroleum ether/ethyl acetate) provided *tert*-butyl 4-(3-((4-cyanopyridin-2-yl)amino)-1-(3,3-difluorocyclopentyl)-1H-pyrazol-5-yl)piperidine-1-carboxylate (80 mg). To an ice-cooled solution of *tert*-butyl 4-(3-((4-cyanopyridin-2-yl)amino)-1-(3,3-difluorocyclopentyl)-1H-pyrazol-5-yl)piperidine-1-carboxylate (80 mg, 0.17 mmol) in dichloromethane (10 mL) was added 2,2,2-trifluoroacetic acid (3 mL). The mixture was stirred at 23 °C for 3 h and concentrated under reduced pressure. To 2-((1-(3,3-difluorocyclopentyl)-5-(piperidin-4-yl)-1H-pyrazol-3-yl)amino)isonicotinonitrile (65 mg, 0.17 mmol) in methanol (10 mL) was added oxetan-3-one (25 mg, 0.32 mmol) and acetic acid (200  $\mu$ L), and the resulting mixture was stirred at 23 °C for 1 h. Sodium cyanoborohydride (32 mg, 0.51 mmol) was added at 23 °C under nitrogen, and the mixture was stirred at 23 °C for an additional 3 h. The mixture was quenched with water (15 mL) and extracted with ethyl acetate (3 × 20 mL). The combined organic was dried over anhydrous sodium sulfate, concentrated under reduced pressure, and purified by preparative reverse-phase HPLC to afford the title compound as a white solid (10.1 mg, 13.9%). LCMS:  $m/z = 429.0$  [ $M + H$ ]<sup>+</sup>; <sup>1</sup>H NMR (400 MHz, CD<sub>3</sub>OD)  $\delta$  8.27 (d,  $J = 5.2$  Hz, 1H), 7.78 (s, 1H), 6.94 (d,  $J = 4.4$  Hz, 1H), 6.05 (s, 1H), 4.92–4.90 (m, 1H), 4.72–4.69 (m, 2H), 4.64–4.61 (m, 2H), 3.64–3.51 (m, 1H), 2.92–2.87 (m, 2H), 2.81–2.46 (m, 4H), 2.28–2.15 (m, 4H), 2.07–2.00 (m, 2H), 1.94–1.91 (m, 2H), 1.79–1.77 (m, 2H).

2-((5-(1-(Oxetan-3-yl)piperidin-4-yl)-1-(tetrahydrofuran-3-yl)-1H-pyrazol-3-ylamino)isonicotinonitrile (**13**). The title compound (3.4 mg, 3.3% yield) was prepared in a manner analogous to **12** by



substituting *tert*-butyl 4-(3-iodo-1-(tetrahydrofuran-3-yl)-1*H*-pyrazol-5-yl)piperidine-1-carboxylate for *tert*-butyl 4-(1-(3,3-difluorocyclopentyl)-3-iodo-1*H*-pyrazol-5-yl)piperidine-1-carboxylate. LCMS:  $m/z$  = 394.9  $[M + H]^+$ ;  $^1H$  NMR (400 MHz,  $CDCl_3$ )  $\delta$  8.28 (d,  $J$  = 4.8 Hz, 1H), 7.59 (s, 1H), 7.01 (s, 1H), 6.92–6.90 (m, 1H), 5.95 (s, 1H), 4.82–4.70 (m, 1H), 4.69–4.62 (m, 4H), 4.23–4.20 (m, 1H), 4.12–4.09 (m, 1H), 3.94–3.99 (m, 2H), 3.50–3.54 (m, 1H), 2.86–2.89 (m, 2H), 2.60–2.63 (m, 1H), 2.44–2.34 (m, 2H), 1.98–1.79 (m, 6H).

2-((1-(Oxetan-3-yl)piperidin-4-yl)-1-(tetrahydro-2*H*-pyran-4-yl)-1*H*-pyrazol-3-yl)amino)isonicotinonitrile (**14**). A solution of **52** (450 mg, 0.98 mmol), 2-aminoisonicotinonitrile (233 mg, 1.96 mmol),  $N^1,N^2$ -dimethylcyclohexane-1,2-diamine (28 mg, 0.20 mmol), potassium phosphate (623 mg, 2.94 mmol), and copper iodide (38 mg, 0.20 mmol) in  $N,N$ -dimethylformamide (4 mL) was purged with nitrogen and heated at 160 °C under microwave irradiation for 1 h. The mixture was diluted with ethyl acetate (20 mL) and filtered. The filtrate was extracted with ethyl acetate (3  $\times$  20 mL). The collected organic was washed with saturated aqueous sodium chloride solution (20 mL), dried over sodium sulfate, filtered, and concentrated under reduced pressure. Purification by flash column chromatography (3:1 petroleum ether/ethyl acetate) provided intermediate *tert*-butyl 4-(3-((4-cyanopyridin-2-yl)amino)-1-(tetrahydro-2*H*-pyran-4-yl)-1*H*-pyrazol-5-yl)piperidine-1-carboxylate (60 mg, 0.13 mmol) which was dissolved in dichloromethane (10 mL) and 2,2,2-trifluoroacetic acid (3 mL) at 0 °C. The mixture was warmed to 23 °C for 3 h and concentrated under reduced pressure. To a solution of crude 2-((5-(piperidin-4-yl)-1-(tetrahydro-2*H*-pyran-4-yl)-1*H*-pyrazol-3-yl)amino)isonicotinonitrile (46 mg, 0.13 mmol) in methanol (10 mL) was added oxetan-3-one (19 mg, 0.26 mmol) and acetic acid (200  $\mu$ L). The mixture was heated to 60 °C for 1 h. Sodium cyanoborohydride (25 mg, 0.39 mmol) was under nitrogen, and the mixture was heated at 60 °C for another 3 h. The mixture was quenched with water (15 mL) and extracted with ethyl acetate (3  $\times$  20 mL). The combined organic was dried over anhydrous sodium sulfate and concentrated under reduced pressure. Purification by preparative reverse-phase HPLC afforded the title compound as a white solid (15 mg, 28% yield). LC/MS:  $m/z$  = 409.15  $[M + H]^+$ ;  $^1H$  NMR (400 MHz,  $CD_3OD$ )  $\delta$  8.27 (d,  $J$  = 5.2 Hz, 1H), 7.69 (s, 1H), 6.94 (d,  $J$  = 5.2 Hz, 1H), 6.07 (s, 1H), 4.74–4.70 (m, 2H), 4.65–4.62 (m, 2H), 4.39–4.34 (m, 1H), 4.10–4.06 (m, 2H), 3.65–3.54 (m, 3H), 2.92–2.80 (m, 3H), 2.35–2.25 (m, 2H), 2.08–2.02 (m, 2H), 1.96–1.93 (m, 2H), 1.83–1.77 (m, 5H).

2-(1-(Cyclobutylmethyl)-5-(1-(oxetan-3-yl)piperidin-4-yl)-1*H*-pyrazol-3-yl)amino)isonicotinonitrile (**15**). A solution of **41** (100 mg, 0.3 mmol) and oxetan-3-one (43.0 mg, 0.595 mmol) in dichloromethane (2.4 mL) was stirred at 23 °C for 15 min. Sodium triacetoxyborohydride (199 mg, 0.892 mmol) was added, and the resulting suspension was maintained at 23 °C for an additional 1 h. The reaction mixture was partitioned between dichloromethane (15 mL) and saturated aqueous ammonium chloride solution (15 mL). The organic was separated, and the aqueous layer was further extracted with dichloromethane (2  $\times$  5 mL). The collected organic was dried over anhydrous sodium sulfate, filtered, and concentrated under reduced pressure. Purification by preparative reverse-phase HPLC afforded the title compound as a white solid (10 mg, 8%). LCMS:  $m/z$  = 393.3  $[M + H]^+$ ;  $^1H$  NMR (400 MHz,  $DMSO-d_6$ )  $\delta$  9.68 (s, 1H), 8.32 (d,  $J$  = 5.2 Hz, 1H), 7.64 (s, 1H), 7.03 (d,  $J$  = 4.8 Hz, 1H), 6.11 (s, 1H), 4.54 (t,  $J$  = 6.5 Hz, 2H), 4.44 (t,  $J$  = 6.1 Hz, 2H), 3.98 (d,  $J$  = 7.1 Hz, 2H), 3.41 (p,  $J$  = 6.5 Hz, 1H), 2.87–2.58 (m, 4H), 2.05–1.72 (m, 10H), 1.64–1.49 (m, 2H).

2-((1-Cyclopentyl-5-(1-(oxetan-3-yl)azetidin-3-yl)-1*H*-pyrazol-3-yl)amino)isonicotinonitrile (**16**). A mixture of **42** (0.080 g, 0.26 mmol) and oxetan-3-one (37 mg, 0.52 mmol) in dichloromethane (3 mL) was stirred at 23 °C for 15 min. Sodium triacetoxyborohydride (49 mg, 0.78 mmol) was added at 23 °C. After 1 h, the reaction mixture was partitioned between dichloromethane (15 mL) and saturated aqueous ammonium chloride solution (15 mL). The organic was separated, and the aqueous layer was further extracted with dichloromethane (2  $\times$  5 mL). The collected organic was dried over anhydrous sodium sulfate, filtered, and concentrated under reduced pressure. Purification by preparative reverse-phase HPLC afforded the

title compound as a white solid (24 mg, 25% yield). LCMS:  $m/z$  = 365.0  $[M + H]^+$ ;  $^1H$  NMR (400 MHz,  $CD_3CN$ )  $\delta$  8.28 (d,  $J$  = 5.2 Hz, 1H), 8.08 (s, 1H), 7.79 (s, 1H), 6.97 (d,  $J$  = 5.2 Hz, 1H), 6.11 (s, 1H), 4.65 (t,  $J$  = 6.8 Hz, 2H), 4.47–4.44 (m, 3H), 3.90–3.87 (m, 4H), 3.40 (s, 2H), 2.00–1.93 (m, 3H), 1.91–1.88 (m, 3H), 1.69–1.65 (m, 2H).

2-((1-Cyclopentyl-5-(1-(oxetan-3-yl)pyrrolidin-3-yl)-1*H*-pyrazol-3-yl)amino)isonicotinonitrile (**17**). The title compound (15 mg, 16%) was prepared in a manner analogous to **14** by substituting *tert*-butyl 3-(1-cyclopentyl-3-iodo-1*H*-pyrazol-5-yl)pyrrolidine-1-carboxylate for *tert*-butyl 4-(3-iodo-1-(tetrahydro-2*H*-pyran-4-yl)-1*H*-pyrazol-5-yl)piperidine-1-carboxylate. LCMS:  $m/z$  = 378.9  $[M + H]^+$ ;  $^1H$  NMR (400 MHz,  $CD_3OD$ )  $\delta$  8.24 (d,  $J$  = 5.2 Hz, 1H), 7.70 (s, 1H), 6.92 (d,  $J$  = 5.2 Hz, 1H), 6.08 (s, 1H), 4.77–4.71 (m, 2H), 4.66–4.61 (m, 2H), 3.76–3.73 (m, 1H), 3.57–3.53 (m, 1H), 3.12–3.07 (m, 1H), 2.85–2.79 (m, 1H), 2.68–2.62 (m, 1H), 2.54–2.49 (m, 1H), 2.40–2.35 (m, 1H), 2.06–1.88 (m, 9H), 1.73–1.69 (m, 2H).

2-((1-Cyclopentyl-5-(tetrahydrofuran-3-yl)-1*H*-pyrazol-3-yl)amino)isonicotinonitrile (**18**). To a suspension of **54** (160 mg, 0.48 mmol), 2-aminoisonicotinonitrile (75 mg, 0.63 mmol),  $N^1,N^2$ -dimethylcyclohexane-1,2-diamine (34 mg, 0.24 mmol), potassium phosphate (102 mg, 0.48 mmol), and copper iodide (46 mg, 0.24 mmol) in  $N,N$ -dimethylformamide (3 mL) was purged with nitrogen and heated at 160 °C under microwave irradiation for 1 h. The mixture was diluted with ethyl acetate (20 mL) and filtered. The filtrate was extracted with ethyl acetate (2  $\times$  20 mL), and the collected organic was washed with saturated aqueous sodium chloride solution (20 mL), dried over sodium sulfate, filtered, and concentrated under reduced pressure. Purification by preparative reverse-phase HPLC afforded the title compound as white solid (11 mg, 7%). LCMS:  $m/z$  = 324.0  $[M + H]^+$ ;  $^1H$  NMR (400 MHz,  $CD_3OD$ )  $\delta$  8.41 (d,  $J$  = 6.8 Hz, 1H), 7.67 (s, 1H), 7.28 (d,  $J$  = 6.8 Hz, 1H), 6.05 (s, 1H), 4.83–4.80 (m, 1H), 4.13–4.09 (m, 1H), 4.02–3.97 (m, 1H), 3.93–3.87 (m, 1H), 3.77–3.67 (m, 2H), 2.48–2.40 (m, 1H), 2.16–2.09 (m, 5H), 2.02–1.96 (m, 3H), 1.81–1.72 (m, 2H).

2-((4-Cyclopropyl-5-(1-(oxetan-3-yl)piperidin-4-yl)thiazol-2-yl)amino)isonicotinonitrile (**19**). A mixture of **61** (0.10 g, 0.36 mmol), 2-chloroisonicotinonitrile (0.050 g, 0.36 mmol), potassium phosphate (0.230 g, 1.08 mmol), and  $Pd(t-Bu_3P)_2$  (0.010 mg, 0.020 mmol) in 1,4-dioxane (5 mL) was stirred at 100 °C for 3 h. After cooling to 23 °C, the mixture was extracted with ethyl acetate (2  $\times$  30 mL). The collected organic was washed with brine (50 mL), dried over sodium sulfate, filtered, and concentrated under reduced pressure. The residue was purified by preparative reverse-phase HPLC to afford the title compound as white solid (7 mg, 5%). LCMS:  $m/z$  = 382.2  $[M + H]^+$ ;  $^1H$  NMR (400 MHz,  $CD_3OD$ )  $\delta$  8.42 (d,  $J$  = 4.0 Hz, 1H), 7.27 (s, 1H), 7.07–7.06 (m, 1H), 4.76–4.72 (m, 2H), 4.69–4.65 (m, 2H), 3.76–3.69 (m, 1H), 3.31–3.11 (m, 1H), 3.05–3.02 (m, 2H), 2.26–2.21 (m, 2H), 2.05–2.02 (m, 2H), 1.93–1.78 (m, 4H), 0.95–0.75 (m, 4H).

2-((2-Cyclopentyl-1-(1-(oxetan-3-yl)piperidin-4-yl)-1*H*-imidazol-4-yl)amino)isonicotinonitrile (**20**). The title compound (3.5 mg, 7.9%) was prepared in a manner analogous to **14** by substituting *tert*-butyl 4-(2-cyclopentyl-4-iodo-1*H*-imidazol-1-yl)piperidine-1-carboxylate for *tert*-butyl 4-(3-iodo-1-(tetrahydro-2*H*-pyran-4-yl)-1*H*-pyrazol-5-yl)piperidine-1-carboxylate. LCMS:  $m/z$  = 393.0  $[M + H]^+$ ;  $^1H$  NMR (400 MHz,  $CD_3OD$ )  $\delta$  8.27 (d,  $J$  = 5.2 Hz, 1H), 7.24 (s, 1H), 7.04 (s, 1H), 6.88–6.87 (m, 1H), 4.74–4.70 (m, 2H), 4.64–4.61 (m, 2H), 4.18–4.16 (m, 1H), 3.60–3.56 (m, 1H), 3.27–3.25 (m, 1H), 2.96–2.93 (m, 2H), 2.13–2.00 (m, 9H), 1.87–1.84 (m, 4H), 1.72–1.69 (m, 2H).

*tert*-Butyl 4-(2-Cyanoacetyl)piperidine-1-carboxylate (**25**). To a stirred solution of 1-*tert*-butyl 4-methylpiperidine-1,4-dicarboxylate (**21**) (50.0 g, 206 mmol) in THF (1 L) was added acetonitrile (53.0 mL, 103 mmol). The reaction was cooled to 0 °C and potassium *tert*-butoxide (69.0 g, 616 mmol) was added portion-wise. The resulting mixture was stirred at 23 °C for 1 h. The reaction mixture was quenched with saturated ammonium chloride (2 L) and extracted with ethyl acetate (3  $\times$  500 mL). The collected organic was sequentially washed with saturated aqueous sodium chloride solution, dried over sodium sulfate, filtered, and concentrated under reduced pressure to

afford the title compound as a pale yellow oil (40 g, 77% crude yield). TLC ( $R_f$  = 0.5 in 2:1 petroleum ether/ethyl acetate).

**tert-Butyl 3-(2-Cyanoacetyl)azetidine-1-carboxylate (26).** To an ice-cooled solution of 1-*tert*-butyl 3-methyl azetidine-1,3-dicarboxylate (22) (10.0 g, 46.5 mmol) and acetonitrile (2.90 g, 69.8 mmol) in tetrahydrofuran (250 mL) was added potassium *tert*-butoxide (7.83 g, 69.8 mmol) portion-wise. The resulting mixture was warmed to 23 °C. After 1 h, the reaction mixture was quenched with saturated aqueous ammonium chloride solution (1 L), and the resulting solution was extracted with ethyl acetate (3 × 400 mL). The combined organic was washed with saturated aqueous sodium chloride solution (2 × 300 mL), dried over sodium sulfate, and concentrated under reduced pressure to afford the title compound as a light yellow solid (10 g, 96% crude yield) which was used without further purification.

**tert-Butyl 3-(2-Cyanoacetyl)pyrrolidine-1-carboxylate (27).** To an ice-cooled solution of 1-*tert*-butyl 3-methyl pyrrolidine-1,3-dicarboxylate (23) (22.0 g, 96.1 mmol) and acetonitrile (21.0 mL, 480 mmol) in tetrahydrofuran (440 mL) was added potassium *tert*-butoxide (32.3 g, 288 mmol) portion-wise. The resulting mixture was warmed to 23 °C and stirred for 1.5 h. The reaction mixture was quenched with saturated aqueous ammonium chloride solution (1 L), and the resulting mixture was extracted with ethyl acetate (3 × 500 mL). The collected organic was washed with saturated aqueous sodium chloride solution (2 × 500 mL), dried over sodium sulfate, filtered, and concentrated under reduced pressure to afford the title compound as a light yellow solid (0.020 kg, 88% crude yield). LCMS:  $m/z$  = 239.1 [ $M + H$ ]<sup>+</sup>.

**3-Oxo-3-(tetrahydrofuran-3-yl)propanenitrile (28).** To an ice-cooled solution of methyl tetrahydrofuran-3-carboxylate (24) (50.0 g, 0.385 mol) and acetonitrile (47.0 g, 1.15 mol) in tetrahydrofuran (500 mL) was added potassium *tert*-butoxide (129 g, 1.15 mol) portion-wise. The resulting mixture was warmed to 23 °C and stirred for 1 h. The reaction mixture was quenched with saturated aqueous ammonium chloride solution (1 L), and the resulting solution was extracted with ethyl acetate (3 × 400 mL). The collected organic was washed with saturated aqueous sodium chloride solution (400 mL), dried over sodium sulfate, filtered, and concentrated under reduced pressure to afford the title compound (41 g, 77% crude yield).

**tert-Butyl 4-(3-Amino-1H-pyrazol-5-yl)piperidine-1-carboxylate (29).** To a solution of 25 (40.0 g, 158 mmol) was added hydrazine monohydrate (39.6 mL, 792 mmol) in 2-propanol (500 mL) and heated at 80 °C for 18 h. The reaction mixture was concentrated under reduced pressure, and the resulting residue was dissolved in dichloromethane (1 L). The solution was washed sequentially with water (500 mL) and saturated aqueous sodium chloride solution (500 mL). The collected organic layer was dried over anhydrous sodium sulfate, filtered, and concentrated under reduced pressure to afford the title compound as a yellow oil (35 g, 83% crude yield). LCMS:  $m/z$  = 267.2 [ $M + H$ ]<sup>+</sup>; <sup>1</sup>H NMR (400 MHz, DMSO-*d*<sub>6</sub>): δ 11.14 (br s, 1 H), 5.15 (s, 1 H), 4.41 (br s, 2 H), 3.93–3.90 (m, 2 H), 2.76–2.74 (m, 2 H), 2.65–2.55 (m, 1 H), 1.78–1.74 (m, 2 H), 1.39–1.36 (m, 11 H).

**tert-Butyl 3-(3-Amino-1H-pyrazol-5-yl)azetidine-1-carboxylate (30).** A solution of 26 (10.0 g, 44.6 mol, crude) and hydrazine monohydrate (40 mL) in isopropyl alcohol (200 mL) was heated at 80 °C for 16 h. After removal of the solvent under reduced pressure, the resulting residue was redissolved in dichloromethane (500 mL). The organic solution was washed sequentially with water (500 mL) and saturated aqueous sodium chloride solution (500 mL). The collected organic was dried over sodium sulfate and concentrated under reduced pressure to afford the title compound as a yellow solid (10 g, 94% crude yield). LCMS:  $m/z$  = 238.9 [ $M + H$ ]<sup>+</sup>; <sup>1</sup>H NMR (400 MHz, DMSO-*d*<sub>6</sub>): δ 11.30 (br s, 1H), 5.28 (s, 1H), 4.68 (br s, 2H), 4.12–4.08 (m, 2H), 3.90–3.79 (m, 2H), 3.63–3.56 (m, 1H), 1.38 (s, 9H).

**tert-Butyl 3-(3-Amino-1H-pyrazol-5-yl)pyrrolidine-1-carboxylate (31).** A solution of 27 (16.5 g, 69.3 mmol, crude) and hydrazine monohydrate (19.0 mL, 347 mmol) in isopropyl alcohol (400 mL) was heated to 80 °C for 16 h. After removal of the solvent under reduced pressure, the residue was redissolved in dichloromethane (500 mL). The organic solution was washed sequentially with water (500 mL) and saturated aqueous sodium chloride solution (500 mL), dried

over sodium sulfate, and concentrated under reduced pressure to afford the title compound as a yellow solid (15.8 g, 90% crude yield). LCMS:  $m/z$  = 253.1 [ $M + H$ ]<sup>+</sup>.

**5-(Tetrahydrofuran-3-yl)-1H-pyrazol-3-amine (32).** To a stirred solution of 28 (41.0 g, 0.295 mol) in 2-propanol (400 mL) was added hydrazine monohydrate (44.2 g, 0.885 mol), and the mixture was heated at 80 °C for 10 h. The reaction mixture was concentrated under reduced pressure, and the resulting residue was dissolved in dichloromethane (500 mL). The organic solution was sequentially washed with water (3 × 150 mL) and saturated aqueous sodium chloride solution (200 mL). The collected organic was dried over sodium sulfate, filtered, and concentrated under reduced pressure to afford the title compound as a yellow solid (38.5 g, 85% crude yield). LCMS:  $m/z$  = 153.8 [ $M + H$ ]<sup>+</sup>.

**tert-Butyl 4-(3-(1,3-Dioxoisindolin-2-yl)-1H-pyrazol-5-yl)piperidine-1-carboxylate (33).** To a stirred solution of 29 (35.0 g, 131 mmol) in dioxane (700 mL) was added phthalic anhydride (19.4 g, 131 mmol). The resulting reaction mixture was heated at 90 °C for 18 h. The reaction mixture was poured into water (2 L) and extracted with ethyl acetate (3 × 1 L). The collected organic was washed with saturated aqueous sodium chloride solution, dried over anhydrous sodium sulfate, filtered, and concentrated under reduced pressure. The resulting pale yellow viscous oil was triturated with ether to afford the title compound as a white solid (40 g, 77%). LCMS:  $m/z$  = 395.3 [ $M - 1$ ]<sup>−</sup>.

**tert-Butyl 3-(5-(1,3-Dioxoisindolin-2-yl)-1H-pyrazol-3-yl)azetidine-1-carboxylate (34).** A solution of crude 30 (2.0 g, 7.9 mmol) and isobenzofuran-1,3-dione (1.2 g, 7.9 mmol) in dioxane (20 mL) was heated at 110 °C for 2 h. The reaction mixture was concentrated under reduced pressure and extracted with ethyl acetate (3 × 80 mL) and water (80 mL). The collected organic was washed with saturated aqueous sodium chloride solution (80 mL), dried over sodium sulfate, filtered, and concentrated under reduced pressure. Purification by flash column chromatography (1:2 petroleum ether/ethyl acetate) afforded the title compound as a white solid (1.5 g, 52%). LCMS:  $m/z$  = 369.0 [ $M + H$ ]<sup>+</sup>.

**tert-Butyl 4-(3-(1,3-Dioxoisindolin-2-yl)-1-isopropyl-1H-pyrazol-5-yl)piperidine-1-carboxylate (35).** A sealed tube charged with 33 (10.0 g, 252 mmol), cesium carbonate (24.6 g, 75.8 mmol) and isopropyl iodide (12.6 mL, 126 mmol) in *N,N*-dimethylformamide (200 mL) was heated at 60 °C for 3 h. The reaction mixture was poured into water (100 mL) and extracted with ethyl acetate (3 × 100 mL). The collected organic was washed with saturated aqueous sodium chloride solution, dried over anhydrous sodium sulfate, and concentrated under reduced pressure. Purification by flash column chromatography (4:1 heptane/ethyl acetate) afforded the title compound as a pale white solid (2.2 g, 20%). LCMS:  $m/z$  = 439.5 [ $M + H$ ]<sup>+</sup>.

**tert-Butyl 4-(1-(Cyclobutylmethyl)-3-(1,3-dioxoisindolin-2-yl)-1H-pyrazol-5-yl)piperidine-1-carboxylate (36).** A glass tube charged with 33 (0.500 g, 1.26 mmol), cesium carbonate (823 mg, 2.52 mmol), and (bromomethyl)cyclobutane (376 mg, 2.52 mmol) in *N,N*-dimethylacetamide (10 mL) was sealed and heated at 50 °C for 16 h. The reaction mixture was concentrated under reduced pressure. Purification by flash column chromatography (0% → 100%, heptane/ethyl acetate) afforded the title compound as an off-white solid (312 mg, 53%). LCMS:  $m/z$  = 465.5 [ $M + H$ ]<sup>+</sup>.

**tert-Butyl 3-(1-Cyclopentyl-3-(1,3-dioxoisindolin-2-yl)-1H-pyrazol-5-yl)azetidine-1-carboxylate (37).** A suspension of 34 (1.20 g, 3.26 mmol), bromocyclopentane (970 mg, 6.5 mmol), and cesium carbonate (2.10 g, 6.52 mmol) in *N,N*-dimethylformamide (10 mL) was heated at 100 °C for 3 h under nitrogen. The reaction mixture was diluted with ethyl acetate (50 mL), and the resulting solid precipitate was filtered. The filtrate was concentrated under reduced pressure. Purification by flash column chromatography (3:1 petroleum ether/ethyl acetate) afforded the title compound as a white solid (0.30 g, 21%). LCMS:  $m/z$  = 437.1 [ $M + H$ ]<sup>+</sup>.

**tert-Butyl 4-(3-Amino-1-isopropyl-1H-pyrazol-5-yl)piperidine-1-carboxylate (38).** To an ice-cooled solution of 35 (28.0 g, 63.9 mmol) in methanol (1 L) was added hydrazine hydrate (9.50 mL, 192



mmol). After stirring at 23 °C for 30 min, the reaction mixture was concentrated under reduced pressure. The resulting oil was triturated with ethyl acetate, and the solid was filtered. The filtrate was washed with water and concentrated under reduced pressure. The resulting oil was triturated with ether to afford the title compound as a white solid (10.5 g, 53%). LCMS:  $m/z$  = 309.3  $[M + H]^+$ ;  $^1H$  NMR (400 MHz, DMSO- $d_6$ ):  $\delta$  5.15 (s, 1 H), 4.40 (br s, 2 H), 4.31 (m, 1 H), 4.00 (m, 2 H), 2.70–2.89 (m, 3 H), 1.74 (m, 2 H), 1.41 (s, 9 H), 1.32 (m, 2 H), 1.27 (d, 6 H).

**tert-Butyl 4-(3-Amino-1-(cyclobutylmethyl)-1H-pyrazol-5-yl)piperidine-1-carboxylate (39).** To a solution of **36** (312 mg, 0.672 mmol) in methanol (2.7 mL) was added hydrazine hydrate (103 mg, 2.01 mmol) at 23 °C. After 16 h, the reaction mixture was concentrated under reduced pressure to afford the title compound as a dark yellow oil (224 mg, 99% crude yield). LCMS:  $m/z$  = 335.5  $[M + H]^+$ .

**tert-Butyl 3-(3-Amino-1-cyclopentyl-1H-pyrazol-5-yl)azetidine-1-carboxylate (40).** A mixture of **37** (0.30 g, 0.69 mmol) in ethanol (10 mL), hydrazine monohydrate (10 mL), and water (10 mL) was heated at 110 °C for 2 h. The reaction mixture was concentrated under reduced pressure, and the resulting aqueous solution was extracted with ethyl acetate (3  $\times$  50 mL). The collected organic was concentrated under reduced pressure to afford the title compound as a yellow oil (150 mg, 71% crude yield). LCMS:  $m/z$  = 306.9  $[M + H]^+$ .

**2-((1-(Cyclobutylmethyl)-5-(piperidin-4-yl)-1H-pyrazol-3-yl)amino)isonicotinonitrile (41).** A suspension of **39** (0.200 g, 0.598 mmol), 2-bromoisonicotinonitrile (109 mg, 0.598 mmol), 4,5-bis(diphenylphosphino)-9,9-dimethylxanthene (27 mg, 0.045 mmol), tris(dibenzylideneacetone)dipalladium(0) (28 mg, 0.031 mmol), and sodium *tert*-butoxide (83 mg, 0.84 mmol) in 1,4-dioxane (3.2 mL) was heated at 80 °C for 1 h. The reaction mixture was filtered and diluted with water (5 mL). The resulting solution was extracted with ethyl acetate (2  $\times$  3 mL). The collected organic was concentrated under reduced pressure and purified by preparative reverse-phase HPLC (149 mg, 57%). The isolated compound (149 mg, 0.342 mmol) was dissolved in dichloromethane (2.5 mL) and a 4.0 M solution of 1,4-dioxane (0.8 mL, 3.2 mmol) at 23 °C. After 3 h, the reaction mixture was concentrated under reduced pressure to afford the title compound as a yellow oil (100 mg, 87% crude yield) which was used without further purification. LCMS:  $m/z$  = 337.4  $[M + H]^+$ .

**2-((5-(Azetidin-3-yl)-1-cyclopentyl-1H-pyrazol-3-yl)amino)isonicotinonitrile (42).** The title compound (0.080 g, 78%) was prepared in a manner analogous to **3** by substituting *tert*-butyl 3-(3-amino-1-cyclopentyl-1H-pyrazol-5-yl)azetidine-1-carboxylate and 2-bromoisonicotinonitrile for *tert*-butyl 4-(3-amino-1-isopropyl-1H-pyrazol-5-yl)piperidine-1-carboxylate and 2-bromo-4-(trifluoromethyl)pyridine, respectively. LCMS:  $m/z$  = 308.9  $[M + H]^+$ .

**tert-Butyl 4-(3-(2,5-Dimethyl-1H-pyrrol-1-yl)-1H-pyrazol-5-yl)piperidine-1-carboxylate (43).** To a solution of **29** (1.60 g, 6.01 mmol) in toluene (4 mL) was added 2,5-hexanedione (1.30 g, 11.4 mmol) and magnesium sulfate (0.723 g, 6.01 mmol). The reaction mixture was heated at 40 °C. After 16 h, the reaction was diluted with water (5 mL) and ethyl acetate (5 mL). The resulting mixture was filtered, and the filtrate was concentrated under reduced pressure to afford a yellow oil (2.01 g, 97% crude yield). LCMS:  $m/z$  = 345.3  $[M + H]^+$ ;  $^1H$  NMR (400 MHz, DMSO- $d_6$ ):  $\delta$  12.66 (s, 1H), 6.08 (s, 1H), 5.72 (s, 2H), 4.11–3.90 (m, 2H), 2.95–2.76 (m, 3H), 2.01 (s, 6H), 1.96–1.86 (m, 2H), 1.58–1.43 (m, 2H), 1.41 (s, 9H).

**tert-Butyl 4-(1-Cyclopentyl-3-(2,5-dimethyl-1H-pyrrol-1-yl)-1H-pyrazol-5-yl)piperidine-1-carboxylate (44).** To a solution of **43** (2.0 g, 5.8 mmol) in *N,N*-dimethylacetamide (48 mL) was added iodocyclopentane (2.4 g, 12 mmol) and cesium carbonate (5.9 g, 18 mmol), and the mixture was heated at 50 °C for 16 h. The reaction mixture was diluted with water (50 mL) and extracted with ethyl acetate (3  $\times$  50 mL). The collected organic was washed with water (20 mL), saturated aqueous sodium chloride solution (20 mL), and concentrated under reduced pressure. Purification by flash column chromatography (0  $\rightarrow$  100% heptane/ethyl acetate) afforded the title

compound as a yellow oil (1.65 g, 69%). LCMS:  $m/z$  = 413.4  $[M + H]^+$ .

**tert-Butyl 4-(3-Amino-1-cyclopentyl-1H-pyrazol-5-yl)piperidine-1-carboxylate (45).** To a solution of potassium hydroxide (0.516 g, 7.82 mmol) in water (7 mL) and ethanol (17 mL) was added hydroxylamine hydrochloride (1.09 g, 20.0 mmol) and **44** (1.65 g, 4.00 mmol). The mixture was heated at 80 °C. After 16 h, the reaction mixture was filtered and concentrated under reduced pressure. Purification by flash column chromatography (0  $\rightarrow$  100% heptane/ethyl acetate) afforded the title compound as a white solid (457 mg, 34%). LCMS:  $m/z$  = 335.3  $[M + H]^+$ .

**tert-Butyl 4-(3-Iodo-1H-pyrazol-5-yl)piperidine-1-carboxylate (46).** To an ice-cooled solution of **29** (35.5 g, 133 mmol) in acetonitrile/water (5:1, 500 mL) was added *p*-toluenesulfonic acid monohydrate (70.3 g, 414 mmol) and sodium nitrite (17.2 g, 250 mmol). After 30 min, sodium iodide (60.0 g, 400 mmol) in water (85 mL) was added at 0 °C. After 30 min, the reaction mixture was warmed to 23 °C. After 1 h, the reaction mixture was poured into water (1500 mL) and extracted with ethyl acetate (3  $\times$  1500 mL). The combined organic layer was washed with saturated aqueous sodium chloride solution (1000 mL), dried over anhydrous sodium sulfate, filtered, and concentrated under reduced pressure. Purification by flash column chromatography (25% ethyl acetate in petroleum ether) afforded the title compound as a yellow solid (11.4 g, 23% yield).  $^1H$  NMR (400 MHz, CDCl<sub>3</sub>):  $\delta$  6.21 (s, 1H), 4.14–4.12 (m, 2H), 3.10–3.02 (m, 1H), 2.90–2.80 (m, 3H), 1.92–1.89 (m, 2H), 1.62–1.52 (m, 2H), 1.46 (s, 9H).

**tert-Butyl 3-(3-Iodo-1H-pyrazol-5-yl)pyrrolidine-1-carboxylate (47).** To an ice-cooled solution of **31** (5.0 g, 20 mmol) in acetonitrile/water (4:1, 75 mL) was added *p*-toluenesulfonic acid monohydrate (10.2 g, 60.0 mmol) and sodium nitrite (2.8 g, 40 mmol). After 30 min, sodium iodide (9.0 g, 60 mmol) in water (15 mL) was added. After an additional 30 min, the reaction mixture was allowed to warm to 23 °C and stirred for 1 h. The reaction mixture was poured into water (500 mL), and the resulting solution was extracted with ethyl acetate (3  $\times$  500 mL). The collected organic was washed with saturated aqueous sodium chloride solution (500 mL), dried over anhydrous sodium sulfate, filtered, and concentrated under reduced pressure. Purification by flash column chromatography (20% ethyl acetate in petroleum ether) yielded the title compound as a yellow solid (2.9 g, 40% yield). LCMS:  $m/z$  = 364.1  $[M + H]^+$ .

**3-Iodo-5-(tetrahydrofuran-3-yl)-1H-pyrazole (48).** To an ice-cooled solution of **32** (18.0 g, 0.118 mmol) in 5:1 acetonitrile/water (240 mL) was added *p*-toluenesulfonic acid monohydrate (30.0 g, 0.176 mmol) and sodium nitrite (12.2 g, 0.176 mmol). After 30 min, sodium iodide (26.5 g, 0.176 mmol) was slowly added, and the reaction was warmed to 23 °C for 1 h. The reaction mixture was diluted with water (600 mL), and the resulting solution was extracted with ethyl acetate (3  $\times$  300 mL). The collected organic was washed with saturated aqueous sodium chloride solution (500 mL), dried over sodium sulfate, filtered, and concentrated under reduced pressure. Purification of the resulting residue by flash column chromatography (2:1 petroleum ether/ethyl acetate) afforded the title compound as a yellow solid (11 g, 35%).  $^1H$  NMR (400 MHz, CDCl<sub>3</sub>):  $\delta$  10.50 (br s, 1H), 5.73 (s, 1H), 3.99–3.92 (m, 2H), 3.86–3.80 (m, 1H), 3.78–3.72 (m, 1H), 3.50–3.38 (m, 1H), 2.40–2.26 (m, 1H), 1.98–1.95 (m, 1H).

**tert-Butyl 4-(3-Iodo-1-(3-oxocyclopentyl)-1H-pyrazol-5-yl)piperidine-1-carboxylate (49).** To a solution of **46** (6.0 g, 16 mmol) in dichloromethane (200 mL) was added cyclopent-2-enone (3.9 g, 48 mmol) and hafnium chloride (512 mg, 1.60 mmol). The resulting mixture was stirred at 23 °C for 12 h. The mixture was filtered, and the filtrate was concentrated under reduced pressure to afford the title compound as dark yellow oil (7.3 g, 100% crude yield). LCMS:  $m/z$  = 359.8  $[MH-100]^+$ .

**tert-Butyl 4-(1-(3,3-Difluorocyclopentyl)-3-iodo-1H-pyrazol-5-yl)piperidine-1-carboxylate (50).** To a crude mixture of **49** (7.30 g, 15.9 mmol) in dichloromethane (200 mL) was added DAST (15 mL) at 0 °C. The mixture was allowed to warm to 23 °C and stirred for 12 h. Saturated aqueous sodium bicarbonate solution (60 mL) was added dropwise, and the resulting mixture was extracted with petroleum

ether (3 × 80 mL). The collected organic was washed with saturated aqueous sodium chloride solution (80 mL), dried over sodium sulfate, filtered, and concentrated under reduced pressure. Purification by flash column chromatography (4:1 petroleum ether/ethyl acetate) afforded the title compound as a white solid (1.5 g, 20% yield).  $R_f$  = 0.3 in 5:1 petroleum ether/ethyl acetate;  $^1\text{H}$  NMR (400 MHz,  $\text{CDCl}_3$ )  $\delta$  6.14 (s, 1H), 4.69–4.65 (m, 1H), 4.23–4.21 (m, 2H), 2.85–2.77 (m, 3H), 2.73–2.67 (m, 1H), 2.55–2.47 (m, 2H), 2.40–2.35 (m, 1H), 2.26–2.14 (m, 2H), 1.81–1.78 (m, 2H), 1.56–1.53 (m, 2H), 1.47 (s, 9H).

**tert-Butyl 4-(3-Iodo-1-(tetrahydrofuran-3-yl)-1H-pyrazol-5-yl)piperidine-1-carboxylate (51).** To an ice-cooled solution of **46** (2.0 g, 5.3 mmol) in  $N,N$ -dimethylformamide (30 mL) was added sodium hydride (637 mg, 26.5 mmol, 60% in mineral oil). After 15 min, tetrahydrofuran-3-yl methanesulfonate (2.03 g, 12.2 mmol) was added dropwise, and the reaction mixture was allowed to warm to 23 °C. After 1 h, the mixture was heated to 90 °C for 2 h. The reaction mixture was quenched with methanol (20 mL) at 23 °C, and the resulting solution was extracted with ethyl acetate (3 × 60 mL). The combined organic was washed with saturated aqueous sodium chloride solution (300 mL), dried over anhydrous sodium sulfate, filtered, and concentrated under reduced pressure. Purification by flash column chromatography (0 → 30% ethyl acetate in petroleum ether) afforded the title compound as white solid (730 mg, 31% yield).  $R_f$  = 0.3 in 2:1 petroleum ether/ethyl acetate.

**tert-Butyl 4-(3-Iodo-1-(tetrahydro-2H-pyran-4-yl)-1H-pyrazol-5-yl)piperidine-1-carboxylate (52).** To an ice-cooled solution of **46** (1.00 g, 2.65 mmol) in  $N,N$ -dimethylformamide (20 mL) was added sodium hydride (127 mg, 5.30 mmol, 60% in mineral oil). After 30 min, tetrahydro-2H-pyran-4-yl methanesulfonate (954 mg, 5.30 mmol) was added to the reaction, and the mixture was purged with nitrogen and warmed to 60 °C. After 4 h, the reaction was cooled to 23 °C and quenched with methanol (20 mL). The resulting solution was concentrated under reduced pressure. Purification by flash column chromatography (3:1 petroleum ether/ethyl acetate) afforded the title compound as a white solid (450 mg, 38% yield). LCMS:  $m/z$  = 461.9  $[\text{M} + \text{H}]^+$ .

**tert-Butyl 3-(1-Cyclopentyl-3-iodo-1H-pyrazol-5-yl)pyrrolidine-1-carboxylate (53).** A suspension of **47** (1.00 g, 2.75 mmol), bromocyclopentane (820 mg, 5.5 mmol), and cesium carbonate (1.79 g, 5.51 mmol) in  $N,N$ -dimethylformamide (5 mL) was heated at 50 °C for 2 h under nitrogen. The reaction mixture was diluted with ethyl acetate (20 mL), and the resulting precipitate was filtered. The filtrate was concentrated under reduced pressure. Purification by flash column chromatography (3:1 petroleum ether/ethyl acetate) afforded the title compound as a white solid (0.30 g, 25%). LCMS:  $m/z$  = 432.1  $[\text{M} + \text{H}]^+$ .

**1-Cyclopentyl-3-iodo-5-(tetrahydrofuran-3-yl)-1H-pyrazole (54).** A suspension of **48** (0.50 g, 1.9 mmol), bromocyclopentane (840 mg, 5.68 mmol), and potassium carbonate (780 mg, 5.68 mmol) in  $N,N$ -dimethylformamide (10 mL) was heated at 80 °C for 3 h under nitrogen. The reaction mixture was diluted with ethyl acetate (20 mL), and the resulting precipitate was filtered. The filtrate was concentrated under reduced pressure. Purification by flash column chromatography (3:1 petroleum ether/ethyl acetate) afforded the title compound as a white solid (0.20 mg, 32%). LCMS:  $m/z$  = 332.8  $[\text{M} + \text{H}]^+$ .

**tert-Butyl (4-Cyclopropylthiazol-2-yl)carbamate (56).** A neat mixture of 4-cyclopropylthiazol-2-amine (**55**) (2.90 g, 20.7 mmol) and di-*tert*-butyl dicarbonate (45.0 g, 20.7 mmol) was heated at 80 °C for 5 h. Purification by flash column chromatography (4:1 petroleum ether/ethyl acetate) afforded the title compound as a white solid (3.69 g, 74% yield). LCMS:  $m/z$  = 240.8  $[\text{M} + \text{H}]^+$ .

**tert-Butyl (5-Chloro-4-cyclopropylthiazol-2-yl)carbamate (57).** To an ice-cooled solution of **56** (1.00 g, 4.17 mmol) in dichloromethane (20 mL) was added 1-chloropyrrolidine-2,5-dione (563 mg, 4.17 mmol) portion-wise. After 2 h at 0 °C, the mixture was diluted with dichloromethane (50 mL), and the resulting solution was washed with water (3 × 50 mL). The collected organic was dried over sodium sulfate, filtered, and concentrated under reduced pressure. Purification by flash column chromatography (10:1 petroleum ether/ethyl acetate)

afforded the title compound as a yellow oil (980 mg, 85% yield). LCMS:  $m/z$  = 218.8  $[\text{M} - 56]$ .

**tert-Butyl 4-(2-((tert-Butoxycarbonyl)amino)-4-cyclopropylthiazol-5-yl)-5,6-dihydropyridine-1(2H)-carboxylate (58).** A suspension of **57** (0.700 g, 2.55 mmol), *tert*-butyl 4-(4,4,5,5-tetramethyl-1,3,2-dioxaborolan-2-yl)-5,6-dihydropyridine-1(2H)-carboxylate (789 mg, 2.55 mmol), 4,5-bis(diphenylphosphino)-9,9-dimethylxanthene (100 mg, 0.200 mmol), tris(dibenzylideneacetone)dipalladium(0) (70 mg, 0.077 mmol), and sodium carbonate (811 mg, 7.65 mmol) in 3:1 1,4-dioxane/water (20 mL) was stirred at 100 °C for 4 h. After cooling to 23 °C, the mixture was extracted with ethyl acetate (3 × 30 mL). The collected organic layer was washed with brine (50 mL), dried over sodium sulfate, filtered, and concentrated under reduced pressure. Purification by flash column chromatography (10:1 petroleum ether/ethyl acetate) afforded the title compound as brown oil (0.50 g, 47%). LCMS:  $m/z$  = 365.9  $[\text{M} - 56]$ .

**tert-Butyl 4-(2-((tert-Butoxycarbonyl)amino)-4-cyclopropylthiazol-5-yl)piperidine-1-carboxylate (59).** A mixture of **58** (0.50 g, 1.2 mmol) and 10% palladium on carbon (500 mg, 0.470 mmol) in methanol (50 mL) was stirred at 23 °C under hydrogen (55 psi) for 16 h. The reaction mixture was filtered through Celite, and the filtrate was concentrated under reduced pressure to afford the title compound as a white solid (490 mg, 98% crude yield). LCMS:  $m/z$  = 424.2  $[\text{M} + \text{H}]^+$ .

**4-Cyclopropyl-5-(piperidin-4-yl)thiazol-2-amine (60).** To an ice-cooled solution of **59** (0.200 g, 0.474 mmol) in dichloromethane (5 mL) was added 2,2,2-trifluoroacetic acid (1.20 mL, 9.48 mmol) under nitrogen. The reaction mixture was warmed to 23 °C. After 4 h, the reaction mixture was concentrated under reduced pressure to afford the title compound as a yellow solid (118 mg, 100% crude yield). LCMS:  $m/z$  = 223.9  $[\text{M} + \text{H}]^+$ .

**4-Cyclopropyl-5-(1-(oxetan-3-yl)piperidin-4-yl)thiazol-2-amine (61).** A mixture of **60** (0.100 g, 0.448 mmol) and oxetan-3-one (64.0 mg, 0.897 mmol) in methanol (5.0 mL) was stirred at 23 °C for 1 h. Sodium cyanoborohydride (83.0 mg, 1.34 mmol) was added, and the reaction was maintained at 23 °C for an additional 3 h. Water (20 mL) was added, and the mixture was extracted with dichloromethane (2 × 20 mL). The collected organic was washed with brine (50 mL), dried over sodium sulfate, filtered, and concentrated under reduced pressure to afford the title compound as a yellow oil (78 mg, 62% crude yield), which was used without further purification. LCMS:  $m/z$  = 280.0  $[\text{M} + \text{H}]^+$ .

**2-Cyclopentyl-4,5-diiodo-1H-imidazole (63).** To a solution of 2-cyclopentyl-1H-imidazole (**62**) (2.00 g, 14.6 mmol) in chloroform (30 mL) was added iodine (3.73 g, 29.2 mmol) and followed by a 4 M solution of sodium hydroxide (30 mL). The mixture was heated at 50 °C for 6 h. After cooling to 23 °C, the reaction was quenched with saturated sodium sulfite solution (50 mL). The organic layer was concentrated under reduced pressure to afford the title compound (2.0 g, 35% crude yield). LCMS:  $m/z$  = 389.1  $[\text{M} + \text{H}]^+$ .

**2-Cyclopentyl-4-iodo-1H-imidazole (64).** To a solution of **63** (2.0 g, 5.2 mmol) in 30% ethanol (30 mL) was added sodium sulfite (1.30 g, 10.4 mmol), and the mixture was refluxed for 10 h. The reaction mixture was concentrated under reduced pressure, and the residue was purified by flash column chromatography (4:1 petroleum ether/ethyl acetate) to afford the title compound as a white solid (1.0 g, 74%). LCMS:  $m/z$  = 263.8  $[\text{M} + \text{H}]^+$ .

**tert-Butyl 4-(2-Cyclopentyl-4-iodo-1H-imidazol-1-yl)piperidine-1-carboxylate (65).** To an ice-cooled solution of **64** (1.0 g, 3.8 mmol) in  $N,N$ -dimethylformamide (20 mL) was added sodium hydride (304 mg, 7.60 mmol, 60% in mineral oil). The reaction mixture was warmed to 23 °C for 30 min before the addition of *tert*-butyl 4-((methylsulfonyl)oxy)piperidine-1-carboxylate (3.20 g, 11.4 mmol). The reaction was purged with nitrogen and heated at 100 °C for 8 h. After cooling to 23 °C, methanol was added to the reaction, and the resulting solution was concentrated under reduced pressure. Purification by preparative reverse-phase HPLC afforded the title compound as a white solid (130 mg, 8%). LCMS:  $m/z$  = 446.1  $[\text{M} + \text{H}]^+$ .  $^1\text{H}$  NMR (400 MHz,  $\text{CDCl}_3$ )  $\delta$  6.92 (s, 1H), 4.40–4.20 (m, 2H),



4.15–4.00 (m, 1H), 3.05–2.92 (m, 1H), 2.90–2.70 (m, 2H), 1.99–1.63 (m, 12H), 1.48 (s, 9H).

## ■ ASSOCIATED CONTENT

### Supporting Information

The Supporting Information is available free of charge on the ACS Publications website at DOI: 10.1021/acs.jmedchem.5b01072.

Protein expression, purification, and crystallographic methods; structure determination and refinement methods; crystal structure data collection and refinement statistics and computational methods for lowest energy conformation analysis (PDF) (CSV)

### Accession Codes

The PDB codes are as follows: 5CEN for Apo DLK kinase domain, 5CEO for **2** complexed with DLK, 5CEP for **3** complexed with DLK, and 5CEQ for **11** complexed with DLK.

## ■ AUTHOR INFORMATION

### Corresponding Authors

\*S.P.: phone, 650-225-4272; e-mail, [patel.snahel@gene.com](mailto:patel.snahel@gene.com).

\*S.F.H.: phone, 650-467-5187; e-mail, [harris.seth@gene.com](mailto:harris.seth@gene.com).

### Present Addresses

○College of Pharmacy, Chungnam National University, 99 Daehak-ro, Yuseong-gu, Daejeon 305–764, Republic of Korea (South)

◆Well Institute for Cell & Molecular Biology, Cornell University, Ithaca, New York, United States

### Notes

The authors declare no competing financial interest.

## ■ ACKNOWLEDGMENTS

We thank the following individuals for their contributions: Mengling Wong, Chris Hamman, and Michael Hayes for compound purification; Genentech protein expression group for the supply of protein; Emile Plise and Jonathan Cheong for MDR1-MDCK data; Xiaolin Zhang, Allan Jauchico, and Xiao Ding for bioanalytical data; Amy Sambrone for formulations work; York Rudhard and the Evotec team for biochemical and cell-based potency data; Wuxi for support with analog synthesis; and Genentech compound management for sample handling.

## ■ ABBREVIATIONS

clogP, calculated logarithm of partition coefficient; CNS MPO, central nervous system multiparameter optimization; DMEM, Dulbecco's modified eagle medium; DLK, dual leucine zipper kinase; DRG, dorsal root ganglion; DAST, diethylaminosulfur trifluoride; ELISA, enzyme-linked immunosorbent assay; JNK, c-Jun N-terminal kinase; LipE, lipophilic ligand efficiency; MAP3K12, mitogen-activated protein kinase kinase kinase 12; MCT, methylcellulose Tween 80; MKK, mitogen-activated protein kinase kinase; MLK, mixed-lineage kinase; MDR1, multidrug resistance protein 1; MDCK, Madin–Darby canine kidney; MSD, mesoscale discovery detection; NGF, nerve growth factor; P-gp, P-glycoprotein

## ■ REFERENCES

(1) Borsello, T.; Forloni, G. JNK signalling: a possible target to prevent neurodegeneration. *Curr. Pharm. Des.* **2007**, *13*, 1875–1886.

(2) Manning, A. M.; Davis, R. J. Targeting JNK for therapeutic benefit: from junk to gold? *Nat. Rev. Drug Discovery* **2003**, *2*, 554–565.

(3) Hirai, S.; Kawaguchi, A.; Suenaga, J.; Ono, M.; Cui, D. F.; Ohno, S. Expression of MUK/DLK/ZPK, an activator of the JNK pathway, in the nervous systems of the developing mouse embryo. *Gene Expression Patterns* **2005**, *5*, 517–523.

(4) Holzman, L. B.; Merritt, S. E.; Fan, G. Identification, molecular cloning, and characterization of dual leucine zipper bearing kinase. A novel serine/threonine protein kinase that defines a second subfamily of mixed lineage kinases. *J. Biol. Chem.* **1994**, *269*, 30808–30817.

(5) Ghosh, A. S.; Wang, B.; Pozniak, C. D.; Chen, M.; Watts, R. J.; Lewcock, J. W. DLK induces developmental neuronal degeneration via selective regulation of proapoptotic JNK activity. *J. Cell Biol.* **2011**, *194*, 751–764.

(6) Pozniak, C. D.; Sengupta Ghosh, A.; Gogineni, A.; Hanson, J. E.; Lee, S. H.; Larson, J. L.; Solanoy, H.; Bustos, D.; Li, H.; Ngu, H.; Jubbs, A. M.; Ayalon, G.; Wu, J.; Scarce-Levie, K.; Zhou, Q.; Weimer, R. M.; Kirkpatrick, D. S.; Lewcock, J. W. Dual leucine zipper kinase is required for excitotoxicity-induced neuronal degeneration. *J. Exp. Med.* **2013**, *210*, 2553–2567.

(7) Chen, X.; Rzhetskaya, M.; Kareva, T.; Bland, R.; During, M. J.; Tank, A. W.; Kholodilov, N.; Burke, R. E. Antiapoptotic and trophic effects of dominant-negative forms of dual leucine zipper kinase in dopamine neurons of the substantia nigra in vivo. *J. Neurosci.* **2008**, *28*, 672–680.

(8) Watkins, T. A.; Wang, B.; Huntwork-Rodriguez, S.; Yang, J.; Jiang, Z.; Eastham-Anderson, J.; Modrusan, Z.; Kaminker, J. S.; Tessier-Lavigne, M.; Lewcock, J. W. DLK initiates a transcriptional program that couples apoptotic and regenerative responses to axonal injury. *Proc. Natl. Acad. Sci. U. S. A.* **2013**, *110*, 4039–4044.

(9) Welsbie, D. S.; Yang, Z.; Ge, Y.; Mitchell, K. L.; Zhou, X.; Martin, S. E.; Berlinicke, C. A.; Hackler, L., Jr.; Fuller, J.; Fu, J.; Cao, L. H.; Han, B.; Auld, D.; Xue, T.; Hirai, S.; Germain, L.; Simard-Bisson, C.; Blouin, R.; Nguyen, J. V.; Davis, C. H.; Enke, R. A.; Boye, S. L.; Merbs, S. L.; Marsh-Armstrong, N.; Hauswirth, W. W.; DiAntonio, A.; Nickells, R. W.; Inglese, J.; Hanes, J.; Yau, K. W.; Quigley, H. A.; Zack, D. J. Functional genomic screening identifies dual leucine zipper kinase as a key mediator of retinal ganglion cell death. *Proc. Natl. Acad. Sci. U. S. A.* **2013**, *110*, 4045–4050.

(10) Huntwork-Rodriguez, S.; Wang, B.; Watkins, T.; Ghosh, A. S.; Pozniak, C. D.; Bustos, D.; Newton, K.; Kirkpatrick, D. S.; Lewcock, J. W. JNK-mediated phosphorylation of DLK suppresses its ubiquitination to promote neuronal apoptosis. *J. Cell Biol.* **2013**, *202*, 747–763.

(11) Miller, B. R.; Press, C.; Daniels, R. W.; Sasaki, Y.; Milbrandt, J.; DiAntonio, A. A dual leucine kinase-dependent axon self-destruction program promotes Wallerian degeneration. *Nat. Neurosci.* **2009**, *12*, 387–389.

(12) Ferraris, D.; Yang, Z.; Welsbie, D. Dual leucine zipper kinase as a therapeutic target for neurodegenerative conditions. *Future Med. Chem.* **2013**, *5*, 1923–34.

(13) Patel, S.; Cohen, F.; Dean, B. J.; De La Torre, K.; Deshmukh, G.; Estrada, A. A.; Ghosh, A. S.; Gibbons, P.; Gustafson, A.; Huestis, M. P.; Le Pichon, C. E.; Lin, H.; Liu, W.; Liu, X.; Liu, Y.; Ly, C. Q.; Lyssikatos, J. P.; Ma, C.; Scarce-Levie, K.; Shin, Y. G.; Solanoy, H.; Stark, K. L.; Wang, J.; Wang, B.; Zhao, X.; Lewcock, J. W.; Siu, M. Discovery of dual leucine zipper kinase (DLK, MAP3K12) inhibitors with activity in neurodegeneration models. *J. Med. Chem.* **2015**, *58*, 401–418.

(14) Sun, H.; Tawa, G.; Wallqvist, A. Classification of scaffold-hopping approaches. *Drug Discovery Today* **2012**, *17*, 310–324.

(15) Bohm, H. J.; Flohr, A.; Stahl, M. Scaffold hopping. *Drug Discovery Today: Technol.* **2004**, *1*, 217–224.

(16) LipE or LLE =  $-\log K_i - \text{clogP}$ . Leeson, P. D.; Springthorpe, B. The influence of drug-like concepts on decision-making in medicinal chemistry. *Nat. Rev. Drug Discovery* **2007**, *6*, 881–890.

(17) Johnson, L. N.; Noble, M. E.; Owen, D. J. Active and inactive protein kinases: structural basis for regulation. *Cell* **1996**, *85*, 149–158.

(18) Huse, M.; Kuriyan, J. The conformational plasticity of protein kinases. *Cell* **2002**, *109*, 275–282.

- (19) Kornev, A. P.; Taylor, S. S.; Ten Eyck, L. F. A helix scaffold for the assembly of active protein kinases. *Proc. Natl. Acad. Sci. U. S. A.* **2008**, *105*, 14377–14382.
- (20) Ryckmans, T.; Edwards, M. P.; Horne, V. A.; Correia, A. M.; Owen, D. R.; Thompson, L. R.; Tran, I.; Tutt, M. F.; Young, T. Rapid assessment of a novel series of selective CB(2) agonists using parallel synthesis protocols: A Lipophilic Efficiency (LipE) analysis. *Bioorg. Med. Chem. Lett.* **2009**, *19*, 4406–4409.
- (21) Bostrom, J.; Berggren, K.; Elebring, T.; Greasley, P. J.; Wilstermann, M. Scaffold hopping, synthesis and structure-activity relationships of 5,6-diaryl-pyrazine-2-amide derivatives: a novel series of CB1 receptor antagonists. *Bioorg. Med. Chem.* **2007**, *15*, 4077–4084.
- (22) St Jean, D. J., Jr.; Fotsch, C. Mitigating heterocycle metabolism in drug discovery. *J. Med. Chem.* **2012**, *55*, 6002–6020.
- (23) ROCS 3.2.0.4; OpenEye Scientific Software: Santa Fe, NM. <http://www.eyesopen.com> (Accessed June 26, 2015).
- (24) Hawkins, P. C.; Skillman, A. G.; Nicholls, A. Comparison of shape-matching and docking as virtual screening tools. *J. Med. Chem.* **2007**, *50*, 74–82.
- (25) Wager, T. T.; Hou, X.; Verhoest, P. R.; Villalobos, A. Moving beyond rules: the development of a central nervous system multiparameter optimization (CNS MPO) approach to enable alignment of druglike properties. *ACS Chem. Neurosci.* **2010**, *1*, 435–449.
- (26) Wager, T. T.; Chandrasekaran, R. Y.; Hou, X.; Troutman, M. D.; Verhoest, P. R.; Villalobos, A.; Will, Y. Defining desirable central nervous system drug space through the alignment of molecular properties, in vitro ADME, and safety attributes. *ACS Chem. Neurosci.* **2010**, *1*, 420–434.
- (27) Gallo, K. A.; Johnson, G. L. Mixed-lineage kinase control of JNK and p38 MAPK pathways. *Nat. Rev. Mol. Cell Biol.* **2002**, *3*, 663–672.
- (28) Rudhard, Y.; Sengupta Ghosh, A.; Lippert, B.; Bocker, A.; Pedaran, M.; Kramer, J.; Ngu, H.; Foreman, O.; Liu, Y.; Lewcock, J. W. Identification of 12/15-lipoxygenase as a regulator of axon degeneration through high-content screening. *J. Neurosci.* **2015**, *35*, 2927–2941.
- (29) Lei, K.; Nimnual, A.; Zong, W. X.; Kennedy, N. J.; Flavell, R. A.; Thompson, C. B.; Bar-Sagi, D.; Davis, R. J. The Bax Subfamily of Bcl2-Related Proteins Is Essential for Apoptotic Signal Transduction by c-Jun NH2-Terminal Kinase. *Mol. Cell. Biol.* **2002**, *22*, 4929–4942.
- (30) Kawatsura, M.; Aburatani, S.; Uenishi, J. Catalytic conjugate addition of heterocyclic compounds to  $\alpha,\beta$ -unsaturated carbonyl compounds by hafnium salts and scandium salts. *Tetrahedron* **2007**, *63*, 4172–4177.
- (31) Klapars, A.; Antilla, J. C.; Huang, X.; Buchwald, S. L. A general and efficient copper catalyst for the amidation of aryl halides and the N-arylation of nitrogen heterocycles. *J. Am. Chem. Soc.* **2001**, *123*, 7727–7729.
- (32) Wolter, M.; Klapars, A.; Buchwald, S. L. Synthesis of N-aryl hydrazides by copper-catalyzed coupling of hydrazides with aryl iodides. *Org. Lett.* **2001**, *3*, 3803–3805.
- (33) Klapars, A.; Huang, X.; Buchwald, S. L. A general and efficient copper catalyst for the amidation of aryl halides. *J. Am. Chem. Soc.* **2002**, *124*, 7421–7428.
- (34) Volkman, J.; Nicholas, K. M. A synthetic quest for tris(imidazolyl) carboxylates and their metal complexes: active site models for quercetin 2,3-dioxygenases and other non-heme redox metalloenzymes. *Tetrahedron* **2012**, *68*, 3368–3376.
- (35) Cohen, F.; Huestis, M.; Ly, C.; Patel, S.; Siu, M.; Zhao, X. Substituted dipyrldylamines and uses thereof. PCT Int. Appl., WO 2013174780, November 28, 2013.
- (36) Chen, M.; Maloney, J. A.; Kallop, D. Y.; Atwal, J. K.; Tam, S. J.; Baer, K.; Kissel, H.; Kaminker, J. S.; Lewcock, J. W.; Weimer, R. M.; Watts, R. J. Spatially coordinated kinase signaling regulates local axon degeneration. *J. Neurosci.* **2012**, *32*, 13439–53.
- (37) ThermoFisher Scientific, Waltham, MA, <http://www.lifetechnologies.com/us/en/home/products-and-services/services/custom-services/screening-and-profiling-services/selectscreen-profiling-service/selectscreen-kinase-profiling-service.html?CID=fl-we113108> (Accessed August 1, 2015).